

***in vivo* tau PET imaging in dementia: pathophysiology, radiotracer quantification, and a systematic review of clinical findings**

Benjamin Hall<sup>1</sup> \*, Elijah Mak<sup>1</sup> \*, Simon Cervenka<sup>1,2</sup>, Franklin I Aigbirhio<sup>3</sup>, James B Rowe<sup>4,5,6</sup>, John T O'Brien<sup>1</sup>

\* Co-first authors, <sup>1</sup> Department of Psychiatry, University of Cambridge School of Clinical Medicine, Cambridge, UK., <sup>2</sup> Department of Clinical Neuroscience, Karolinska Institutet, Stockholm, Sweden, <sup>3</sup> Wolfson Brain Imaging Centre, Department of Clinical Neurosciences, University of Cambridge, UK., <sup>4</sup> Department of Clinical Neurosciences, University of Cambridge, Cambridge, UK., <sup>5</sup> Medical Research Council, Cognition and Brain Sciences Unit, Cambridge, UK., <sup>6</sup> Behavioural and Clinical Neuroscience Institute, University of Cambridge, Cambridge, UK.

Corresponding author:

Prof John O'Brien

Foundation Professor of Old Age Psychiatry

Department of Psychiatry

University of Cambridge School of Clinical Medicine

Box 189, Level E4 Cambridge Biomedical Campus

Cambridge

CB2 0SP

UK

Abstract word count: 316

Manuscript word count: 7687

**ABSTRACT**

In addition to the deposition of  $\beta$ -amyloid plaques, neurofibrillary tangles composed of aggregated hyperphosphorylated tau are one of the pathological hallmarks of Alzheimer's disease and other neurodegenerative disorders. Until now, our understanding about the natural history and topography of tau deposition has only been based on post-mortem and cerebrospinal fluid studies, and evidence continues to implicate tau as a central driver of downstream neurodegenerative processes and cognitive decline. Recently, it has become possible to assess the regional distribution and severity of tau burden *in vivo* with the development of novel radiotracers for positron emission tomography (PET) imaging. In this article, we provide a comprehensive discussion of tau pathophysiology, its quantification with novel PET radiotracers, as well as a systematic review of tau PET imaging in normal aging and various dementia conditions: mild cognitive impairment, Alzheimer's disease, frontotemporal dementia, progressive supranuclear palsy, and Lewy body dementia. We discuss the main findings in relation to group differences, clinical-cognitive correlations of tau PET, and multi-modal relationships among tau PET and other pathological markers. Collectively, the small but growing literature of tau PET has yielded consistent anatomical patterns of tau accumulation that recapitulate post-mortem distribution of neurofibrillary tangles which correlate with cognitive functions and other markers of pathology. In general, AD is characterised by increased tracer retention in the inferior temporal lobe, extending into the frontal and parietal regions in more severe cases. It is also noted that the spatial topography of tau accumulation is markedly distinct to that of amyloid burden in aging and AD. Tau PET imaging has also revealed characteristic spatial patterns among various non-AD tauopathies, supporting its potential role for differential diagnosis. Finally, we propose novel directions for future tau research, including (a) longitudinal imaging in preclinical dementia, (b) multi-modal mapping of tau pathology onto other pathological processes such as

neuroinflammation, and (c) the need for more validation studies against post-mortem samples of the same subjects.

Keywords: dementia; tau; PET; MRI; neurodegeneration; tauopathies; cognitive impairment.

## 1. INTRODUCTION

There are now 30 million people living with dementia world-wide, and the number is expected to rise to 115 million in 2050 (World Alzheimer Report 2010, [www.alz.org](http://www.alz.org)). Alzheimer's disease (AD) is the most common cause making up approximately 60-70%. Other common causes of dementia include vascular dementia, Lewy body dementia (LBD) and frontotemporal dementia (FTD). It is now established that dementia has an insidious latency period, with pathological changes preceding symptom onset by several decades (Trojanowski et al., 2010).

The key neuropathological substrates of AD are tau neurofibrillary tangles (NFTs) and  $\beta$ -amyloid plaques, although activated microglia and cerebrovascular changes also contribute to the overall neuropathological landscape. The 'amyloid cascade hypothesis' posits an initiating event of amyloidosis, with subsequent tau pathology and other downstream processes involving neurotoxicity, synaptic dysfunction, progressive cerebral atrophy and finally cognitive and functional decline (Hardy and Selkoe, 2002). However, the causal role of  $\beta$ -amyloid has been increasingly contested in light of several emerging lines of evidence: (a) approximately 30% of healthy elderly individuals have significant levels of  $\beta$ -amyloid deposition without overt clinical symptoms (Rowe et al., 2010); (b) several anti-amyloid interventions have failed to halt or reverse the disease progression of AD (Karran and Hardy, 2014; Siemers et al., 2015); (c) levels of  $\beta$ -amyloid tend to stagnate by the time of clinical onset and show poor correlations with disease severity (Giannakopoulos et al., 2003). In contrast to the early plateauing of  $\beta$ -amyloid levels, the presence and extent of NFTs and neuronal injury increase in parallel with disease duration and

severity of symptoms (Gómez-Isla et al., 1997). Furthermore, there is convergent evidence that tau, rather than amyloid pathology, is more closely related to memory decline in post-mortem studies of AD (Van Rossum et al., 2012).

Abnormal aggregation of the tau protein is also central to the pathophysiology of other conditions apart from AD, including frontotemporal dementia (FTD) and corticobasal syndrome (CBS), progressive supranuclear palsy (PSP) and to smaller extent in Lewy body dementias (LBDs). Due to overlapping symptoms and neuropathological changes among these conditions, differential diagnosis may be challenging, resulting in sub-optimal therapeutic interventions and inaccurate prognosis. Current approaches that have well-established clinical utility for diagnosis and assessing disease progression in dementia include longitudinal measures of brain atrophy on structural MRI (Frisoni et al., 2010; Mak et al., 2015; see Mak et al., 2016 for a review) and cerebral metabolism using  $^{18}\text{F}$ -fluorodeoxyglucose (FDG-PET) (Firbank et al., 2015; Mosconi, 2013). However, while these imaging measures are highly sensitive to structural and functional changes, they are non-specific markers of synaptic dysfunction, neuronal loss and macroscopic atrophy – all of which are also implicated in other neuropsychiatric diseases such as schizophrenia and late-life depression (Colloby et al., 2012, 2011; Sasamoto et al., 2014). More specific markers of AD would include the levels of  $\beta$ -amyloid ( $\text{A}\beta_{1-42}$ ) and tau (total-tau and phosphorylated-tau<sub>181p</sub>) in the cerebrospinal fluid (CSF) (Agarwal, 2012). However, the procedure is painfully invasive, and CSF measures do not provide spatial information about the distribution of amyloid and tau in the brain. Considering the stereotypical topography of NFTs in AD and regionally-distinct NFTs in other tauopathies (Braak and Braak, 1991; Dickson, 1999), the absence of anatomical localisation in CSF measures makes it less ideal for disease monitoring, evaluation of therapeutic outcomes, and differential diagnosis (i.e. similar overall magnitude of tau may occur in different regions of the brain).

Using molecular imaging techniques such as PET and Pittsburgh Compound B ( $[^{11}\text{C}]\text{PIB}$ ) or other more recently developed fluorine-18 labelled radioligands, it has been possible to characterise amyloid burden *in vivo* for more than a decade (Klunk et al., 2004; O'Brien and Herholz, 2015). In contrast, it was only very recently that PET radiotracers for tau were developed to assess both the regional distribution and the severity of tau pathology (Villemagne et al., 2015). This major scientific advancement could potentially provide a marker of disease progression and aid in the differential diagnosis of neurodegenerative disorders by revealing disease-specific topography of tau deposition.

The purpose of this systematic review is to provide a comprehensive summary of the fast-growing literature of tau PET imaging studies in humans. This paper is divided into two broad sections. We first describe the pathophysiology of tau in dementia, briefly summarise the characteristics of various tau PET tracers as well as methods of quantification, before reviewing the literature of tau PET imaging across multiple dementia conditions. Group comparisons of tau deposition as well as correlations with clinical features and cognitive impairment will be discussed in detail. Finally, directions for future research will be proposed.

## **2. PATHOPHYSIOLOGY OF TAU IN DEMENTIA AND RELATED CONDITIONS**

### ***2.1. Hyperphosphorylation of tau***

Tau is a multi-functional, natively unfolded protein that is located predominantly within axons. Under normal conditions, tau binds to microtubule and provides mechanistic stabilisation (see Wang and Mandelkow, 2015 for a review). Microtubules comprise the cell cytoskeleton and are thus critical for maintaining the cellular structural integrity and axonal transport from the soma to the synaptic terminals. In the human brain, tau exists as six distinct isoforms due to the alternate

mRNA splicing (i.e. exons 2, 3, and 10) of the microtubule associated protein tau (MAPT) gene on chromosome 17, resulting in different numbers of C-terminal repeat sequences: 3-repeat (3R) or 4-repeat (4R) forms. 4R tau isoforms with a fourth microtubule-binding repeat region are encoded by exon 10 while tau mRNAs without exon 10 are transcribed a 3R tau isoform. The healthy adult human cortex has an approximately proportional ratio of 3R and 4R tau isoforms (Spillantini and Goedert, 2013). All six forms of tau are found in AD as opposed to a relative overexpression of 4R tau isoforms in PSP and CBD. The significance of the ratio of the two different isoforms in neurodegenerative diseases is as yet unclear, however it may relate to their differing abilities to stabilize microtubules. The microtubule can switch repeatedly between polymerisation and depolymerisation with rapid shrinking phases. Tau isoforms with 4 repeats shift microtubule dynamics towards assembly by a greater degree than those with 3 repeats. Importantly, the ability of tau to alter microtubule stability is also influenced by post-translational modifications such as phosphorylation. Phosphorylation reduces the affinity of tau for microtubules and thus prevents its stabilising effect, thereby switching towards greater disassembly. Although the understanding of the numerous heterogeneous phosphorylation sites on tau is limited, it has been shown that both 3R and 4R isoforms can produce aggregates and can be phosphorylated at multiple different sites. The resultant change in microtubule dynamics leads to impaired axonal transport in neural cells and the hyperphosphorylated tau aggregates forming structures such as NFTs. The final result of these processes is neuronal dysfunction and cell death (Spillantini and Goedert, 2013; Wang and Mandelkow, 2015).

## **2.2. Tauopathies**

As mentioned, tau pathology is now recognised as a key driver behind various neurodegenerative conditions that are collectively termed as tauopathies. These include AD as well as the broad spectrum of frontotemporal lobar degeneration with tau pathology. These tauopathies differ by

affected brain regions as well as isomeric forms of aggregated tau. There are also ultrastructural distinctions of aggregated tau between AD and non-AD tauopathies. In AD, NFTs typically exist as paired helical filaments, whereas in PSP and CBD, tau filaments are straight. There is also well-established evidence for disease-specific spatial patterns of tau accumulation. In AD, the earliest aggregation of tau are preferentially found in the transentorhinal cortex, before extending widely to the medial and inferior temporal lobe, the parietal regions and the posterior cingulate cortex (Braak and Braak, 1991). This hierarchical pattern is distinct from the midbrain and frontostriatal accumulation found in PSP and CBD respectively (Braak et al., 1992; Dickson, 1999; Williams et al., 2007). In summary, the heterogeneous spatial topography of tau accumulation across various conditions presents a valuable opportunity for clinical differential diagnosis among these tauopathies. In the next section, we provide a brief summary of presently available tau radiotracers and discuss their strengths and weaknesses. For a more in-depth review on the pharmacokinetic characteristics of tau imaging ligands, the readers are directed to another review by Harada and colleagues (Harada et al., 2016).

### **3. DEVELOPMENT AND CHARACTERISTICS OF TAU PET RADIOTRACERS**

#### ***3.1. Challenges of tau imaging***

The robust associations of NFT density with neuronal dysfunction and cognitive impairment have been a strong impetus behind a global effort to develop a PET tracer for *in vivo* imaging of aggregated tau. However, progress for tau tracers has considerably lagged behind its amyloid counterparts due to several challenges: (a) tau is intracellular, thus requiring the ligand to cross the plasma cell membrane and the blood-brain barrier, imposing restrictions on molecular size and lipophilicity; (b) tau neurofibrillary tangles are structurally homologous with  $\beta$ -amyloid aggregates, but are present in lower concentrations, thus requiring tau ligands to have high selectivity (20 – 50 fold affinity) for tau over  $\beta$ -amyloid (Schafer et al., 2012), and finally, (c) the tau protein has

multiple conformations (paired helical filaments vs straight), six isoforms (AD: 3R4R, PSP/FTD: 4R) and numerous post-translational modifications, all of which are factors that could affect sites for ligand binding.

### **3.2. [<sup>18</sup>F]FDDNP**

One of the earliest radioligands developed for tau was [<sup>18</sup>F]FDDNP, which was capable of detecting group differences among healthy controls, MCI, and AD (Barrio et al., 2008; Small et al., 2006). However, it has low selectivity for tau, such that its uptake reflects a combination of amyloid and tau deposition, and therefore its use is limited with respect to tau imaging specifically.

### **3.3. THK compounds**

Okamura and colleagues developed the first tau-selective ligand, [<sup>18</sup>F]THK523, after inspecting a series of quinolone and benzimidazole derivatives that bind preferentially to NFTs over  $\beta$ -amyloid (Okamura et al., 2005). The selectivity of [<sup>18</sup>F]THK523 for phosphorylated tau over  $\beta$ -amyloid was also confirmed in post-mortem studies (Fodero-Tavoletti et al., 2014). The use of [<sup>18</sup>F]THK523 has been validated through a series of *in vitro*, *ex vivo*, and *in vivo* experiments (Fodero-Tavoletti et al., 2011). It possesses fast reversible kinetics and its distribution mirrors the Braak topography of tau in AD (Braak and Braak, 1991). In clinical studies, [<sup>18</sup>F]THK523 binding was shown to be higher in the cortical and hippocampal regions of AD patients compared to age-matched healthy individuals (Villemagne et al., 2014). However, it is not without several limitations. Firstly, [<sup>18</sup>F]THK253 has significant retention within the white matter, limiting accurate quantification of radioligand uptake (Villemagne et al., 2014). Secondly, [<sup>18</sup>F]THK523 does not appear to bind to tau aggregates in non-AD tauopathies such as PSP and CBD (Fodero-Tavoletti et al., 2014). Other THK compounds have since been developed, including [<sup>18</sup>F]THK5105, [<sup>18</sup>F]THK5117 (in the S-form enantiomer also referred to as [<sup>18</sup>F]HK5317 (Chiotis et al., 2016) and [<sup>18</sup>F]THK5351



(Okamura et al., 2013). These ligands have higher affinity for tau compared to [ $^{18}\text{F}$ ]THK523, although substantial white matter binding was still reported for [ $^{18}\text{F}$ ]THK5105 and [ $^{18}\text{F}$ ]THK5117 (Harada et al., 2016). [ $^{18}\text{F}$ ]THK5351 (also known as GE-216) is the latest addition to the arylquinoline series and it shows faster kinetics, lower white matter binding, and consequently higher signal-to-noise ratio compared to [ $^{18}\text{F}$ ]THK5105 and [ $^{18}\text{F}$ ]THK5117 (Harada et al., 2015b).

Previous groups have observed a possible off-target binding of THK compounds to striatal regions such as the basal ganglia (Harada et al., Human Amyloid Imaging 2017). However, there is recent evidence from competition studies suggesting that [ $^{18}\text{F}$ ]THK-5351 may not be selective for tau but also binds to MAO-B sites (Guo et al., Human Amyloid Imaging 2017). A single dose of selegiline (MAO-B inhibitor) resulted in a substantial decrease (36.2 – 51.3%) of [ $^{18}\text{F}$ ]THK5351 uptake among MCI and PSP patients (Ng et al., 2017 Human Amyloid Imaging 2017; Figure 1). Furthermore, there is also new autoradiographic data showing that [ $^{18}\text{F}$ ]THK5351 has lower binding in AD compared to AV-1451, as well as increased off-target binding (Lowe et al., Human Amyloid Imaging 2017). Overall, these recent findings cast doubt on the utility of [ $^{18}\text{F}$ ]THK5351 for clinical use.

### **3.4. [ $^{18}\text{F}$ ]AV-1451**

More recently, benzimidazole pyrimidines derivatives have been identified as promising candidates for application as tau tracers (Xia et al., 2013a). Developed by Kolb and colleagues, [ $^{18}\text{F}$ ]AV1451 (formerly known as T807) is the most widely used tracer at present. Post-mortem studies have shown that [ $^{18}\text{F}$ ]AV1451 binds to tau with 25-fold higher affinity than for  $\beta$ -amyloid or other common protein aggregates (Xia et al., 2013b). The radioligand also has low retention in the white matter thereby facilitating ease of its quantification. Human studies using [ $^{18}\text{F}$ ]AV1451 have

identified binding patterns that parallel with neuropathological stages of tau (Johnson et al., 2016; Ossenkoppele et al., 2016), as well as showing strong correlations with cognitive decline (i.e. episodic memory) and levels of CSF tau (Brier et al., 2016; Chhatwal et al., 2016).

However, there is recent autoradiographic evidence that [ $^{18}\text{F}$ ]AV1451 binding was less evident in non-AD tauopathies (Lowe et al., 2016). In addition, there are reports of substantial off-target binding of [ $^{18}\text{F}$ ]AV1451 in the basal ganglia and the substantia nigra (a brain region known for iron accumulation) in the absence of tau pathology (Lowe et al., 2016). There is also an ongoing debate about [ $^{18}\text{F}$ ]AV1451 binding in the choroid plexus. High retention in the choroid plexus of elderly controls have been attributed to off-target binding (Marquié et al., 2015), although this view has been challenged by recent histological evidence that the epithelial cells of choroid plexus contain tangle-like structures that are morphologically similar to Biondi “ring” tangles (Ikonomic et al., 2016).

### **3.5. [ $^{11}\text{C}$ ]PBB3**

[ $^{11}\text{C}$ ]PBB3 is another tau radiotracer developed by Maruyama and colleagues (Maruyama et al., 2013a). It has 40 – 50 fold higher affinity for NFTs than for amyloid plaques, and possesses good blood-brain barrier penetration and rapid washout (Kimura et al., 2015). As with [ $^{18}\text{F}$ ]AV-1451, there is minimal white matter binding, although non-specific retention has been observed in dural venous sinuses. A notable advantage of this radiotracer compared to its counterparts is its affinity for both the 3R and 4R tau isoforms in several non-AD tauopathies (ie. non-PHF tau conformations), thereby rendering it particularly useful for differential diagnosis on the basis of regional tau topography (Maruyama et al., 2013b). However, the existence of a radiolabelled metabolite entering the brain poses a significant limitation for quantification of [ $^{11}\text{C}$ ]PBB3.

### **3.6. Tracers for the future**

Reflecting the very high pace of developments in the tau PET imaging literature, several novel tracers were recently presented at the Human Amyloid Imaging 2017. In this section, we briefly discuss some of these up and coming tau radiotracers, including Merck's [<sup>18</sup>F]MK-6240, Roche's [<sup>18</sup>F]RO6958948, Genenetch's [<sup>18</sup>F]GTP1 and new analogues of [<sup>11</sup>C]PBB3.

#### **3.6.1. [<sup>18</sup>F]MK-6240**

One of the most promising candidates appears to be the [<sup>18</sup>F]MK-6240 tracer. It has high specificity and selectivity for NFT and as well as good pharmacokinetic properties (Walji et al., 2016). Blocking studies in rhesus monkey also demonstrated no apparent off-target binding, constituting a potential advantage over the widely-used [<sup>18</sup>F]AV1451 (Hostetler et al., 2016). On the basis of these favourable preclinical findings, [<sup>18</sup>F]MK-6240 has been subjected to clinical evaluations in AD patients (Sur et al., Human Amyloid Imaging 2017, Salinas et al., Human Amyloid Imaging 2017). [<sup>18</sup>F]MK-6240 showed a peak brain uptake of ~ 5 SUV and quick washout from all regions in healthy controls, whereas substantial retention was observed in the MTL and expected neocortical regions in AD. Quantitative analyses of dynamic data in 3 AD patients and 3 healthy controls showed good correspondence with standardized uptake ratio (SUV<sub>R</sub>; discussed in Section 4) and MTL uptake was strongly correlated with MMSE ( $R^2 > 0.9$ ) (Salinas et al., Human Amyloid Imaging 2017). Future studies investigating the utility of [<sup>18</sup>F]MK-6240 in non-AD tauopathies are keenly anticipated.

#### **3.6.2. [<sup>18</sup>F]RO6958948**

Developed by Roche, the [<sup>18</sup>F]RO6958948 compound is another high-affinity tau radioligand with desirable clinical profile and kinetic characteristics, such as rapid brain entry and washout, safe metabolic profile and low affinity for amyloid deposits. Preliminary data from a Phase I trial of

[<sup>18</sup>F]RO6958948 showed that it is capable of separating AD patients from controls (Wong et al., 2015). Since then, Wong and colleagues have investigated the longitudinal trajectory (8 – 22 months) of [<sup>18</sup>F]RO6958948 in 4 AD patients. 3 of the 4 AD patients showed significant increase in tau accumulation particularly within Braak-stage regions, highlighting the potential for [<sup>18</sup>F]RO6958948 to track tau progression (Wong et al., Human Amyloid Imaging 2017). Honer and colleagues presented preliminary *in vitro* data directly comparing [<sup>18</sup>F]RO6958948 to [<sup>18</sup>F]AV1451 and [<sup>18</sup>F]THK535, showing that all tracers demonstrated a similar profile of binding to overlapping tau aggregates in AD and non-AD tauopathies. However, none of the tracers showed significant binding to tau pathology in PSP, CBD and Pick's disease (Honer et al., Human Amyloid Imaging 2017).

### 3.6.3. [<sup>18</sup>F] Genentech tau probe 1

The Genentech tau probe 1 (GTP-1) is another tau PET tracer that exhibits desirable pharmacokinetics (Bohorquez et al., Human Amyloid Imaging 2017). Baseline and longitudinal data (6 – 12 months) in AD were recently reported (Weimer et al., Human Amyloid Imaging 2017). At baseline, the authors reported a graded increase in both the intensity (SUVR) and extent (% of suprathreshold voxels) of increased tau pathology as a function of disease severity (prodromal, mild, and moderate AD). Longitudinally, GTP-1 was able to demonstrate progression of tau burden in mild and moderate AD subjects within 6 – 9 months. This pattern contrasted against that of the healthy controls, who showed low baseline tau burden and no longitudinal increase over the follow-up period.

### 3.6.4. Analogues of [<sup>11</sup>C]PBB3

To overcome some of the limitations associated with the [<sup>11</sup>C]PBB3, Shimada and colleagues have developed new fluorinated PBB3 derivatives, such as [<sup>18</sup>F]AM-PBB3 and [<sup>18</sup>F]PM-PBB3

(Shimada et al.; Ono et al., Human Amyloid Imaging 2017). As previously described, the chief disadvantages of the [ $^{11}\text{C}$ ]PBB3 include the short half-life of carbon-11 ( $t_{1/2} = 20$  minutes), significant off-target binding in striatal regions and limited dynamic range. Preliminary examinations of the [ $^{18}\text{F}$ ] PBB3 derivatives in 4 AD patients and 4 age-matched healthy controls showed that AM-PBB3 yielded a 1.5 – 2 fold greater dynamic range than its [ $^{11}\text{C}$ ]based predecessor without substantial off-target signals in the basal ganglia and thalamus (Shimada et al., Human Amyloid Imaging 2017).

### **3.7. The road ahead for tau radiotracers**

It is clear from the plethora of tracers that the field of tau imaging is progressing very rapidly. Nevertheless, there are still unresolved ambiguities about the binding characteristics of some radioligands. The sources of off-target binding may soon be clarified by competition studies (Ng et al., Human Amyloid Imaging 2017), or even resolved by novel tracers that do not have off-target binding (i.e. [ $^{18}\text{F}$ ]MK-6240 and [ $^{18}\text{F}$ ]AM-PBB3). Ultimately, validation of these promising tracers will require cross-comparisons of *in vivo* findings with post-mortem tau quantification. Moving forward, the reproducibility and test-retest reliability of *in vivo* tau quantifications will be a crucial requirement in order for tau imaging to be utilised as (a) surrogate markers of disease monitoring and target engagement in clinical trials, (b) for elucidating the natural history of tau progression and (c) ultimately how it relates to the evolution of cognitive and clinical symptoms across the spectrum of tauopathies.

## **4. QUANTIFICATION OF TAU RADIOLIGAND BINDING**

### **4.1. Standardized uptake value ratios**

In the majority of all clinical PET tau studies published to date, radioligand binding was assessed using SUVR. Briefly, uptake in the target region is normalized by subject weight and injected

radioactivity, and divided with the corresponding value obtained from the cerebellum, which serves as the reference region. Hence, SUVR represents a semi-quantitative estimation of the ratio between total and non-specific binding. This approach is clinically attractive, since there is no arterial sampling, and patient time in the PET system can be limited to a short time frame, typically the interval between 80-100 minutes after injection. However, since radioligand delivery to the brain cannot be controlled for, differences in blood flow may affect SUV values in both target and reference regions. Furthermore, due to lack of true equilibrium, SUVR may show a time-dependent bias relative to quantitative methods, as has been demonstrated e.g. for amyloid radioligands (van Berckel et al., 2013).

#### **4.2. Pharmacokinetic modelling of dynamic data**

Another alternative when a reference region devoid of the target protein can be established is to use the time activity curve (TAC) from this region as input in pharmacokinetic modelling of dynamic data, for instance the simplified reference tissue model (SRTM) (Lammertsma and Hume, 1996) or linear methods e.g. the reference Logan plot (Logan et al., 1996). Ideally, both static and dynamic simplified approaches should be validated using full pharmacokinetic analyses with metabolite-corrected arterial plasma radioactivity as input function (AIF). By using compartmental modelling or graphical methods, quantitative estimates of regional radioligand binding, such as total volume of distribution ( $V_T$ ) or Distribution volume Ratio (DVR) (Logan et al., 1990) (Innis et al., 2007) can be obtained as reference.

Very recently, a limited number of pharmacokinetic modelling papers have emerged for tau radioligands. In a study by Hahn and colleagues, dynamic [ $^{18}\text{F}$ ]AV1451 data and AIF were obtained in 15 control subjects and patients with neurodegenerative disorders (Hahn et al., 2016). AIF Logan showed good correspondence to both SRTM2 and Logan plot ( $R^2=0.92$  and  $0.99$  for

over 80 minutes) as well as SUVr (0.88-0.94 when employing scanning time for over 100 minutes). In a subsequent study, reference Logan showed good correspondence to  $V_T$  obtained using a 2-tissue compartment model ( $R^2 = 0.96$ ) in 4 healthy control subjects, 3 TBI and 4 MCI patients although a negative bias was shown for higher values (Wooten et al., 2016). SUVr showed comparable correspondence and negligible bias ( $R^2 = 0.96$ ). In addition to these AIF-based analyses, Scherbinin et al compared SUVr to reference tissue Logan in 19 individuals, finding high correlations ( $R^2 < 0.86$ ), although a two-fold overestimation was observed using SUVr (Shcherbinin et al., 2016). A time-frame and intensity-dependent bias for SUVr compared to reference tissue models was confirmed also by Baker et al, examining 43 control subjects and AD patients (Baker et al., 2016).

For [ $^{18}\text{F}$ ]THK5117, quantification models were evaluated in 9 subjects with AD or MCI (Jonasson et al., 2016). Both SRTM and reference Logan showed excellent correspondence to AIF Logan, with  $R^2$  values approaching 1, whereas SUVr values were less strongly correlated ( $R^2 = 0.84$ ) and showed a 50% overestimation. Quantification of [ $^{11}\text{C}$ ]CBPP3 was evaluated by Kimura and colleagues in a sample of 14 healthy control subjects and AD patients (Kimura et al., 2015). A dual arterial input function model was employed, since this radioligand has shown to yield a radiolabelled metabolite with blood-brain barrier penetrance (Hashimoto et al., 2014). A graphical analysis showed strong correlations to the MRTM reference tissue model ( $R^2 = 1$ ) as well as SUVr values ( $R^2 = 0.97$ ), however in the latter case there was a time-dependent bias of 5-12%. Furthermore, the brain-penetrant radiometabolite with unknown affinity for tau renders the validation less certain.

### **4.3. Reference regions**

A prerequisite for all reference tissue approaches is that the reference region contains no specific binding and hence can be used as an approximation of non-displaceable volume of distribution ( $V_{ND}$ ). Evidence of lack of cerebellar tau comes in the form of post-mortem studies showing no binding as determined using an *in vitro* binding assay (Marquié et al., 2015). In addition, PET studies have revealed similar kinetics in cerebellum in patients to that of cortical regions in healthy control subjects, with no difference (Wooten et al., 2016) or even higher cerebellar  $V_T$  values in control subjects (Hahn et al., 2016). Although confirmation of the assumption requires demonstrating lack of specific binding as determined *in vivo* using a blocking design, studies performed thus far support the use of cerebellum as reference region for both dynamic and static methods. One exception is dentate nucleus which shows presence of tau in PSP patients both *in vitro* and *in vivo* (Cho et al., 2016c; Smith et al., 2016b; Whitwell et al., 2016), suggesting that this section of cerebellum should be omitted from the reference ROI. In addition, ROIs including superior parts of cerebellum may be contaminated by spill-over effects from neighbouring cortical regions and increase variability in cross-sectional comparisons (Baker et al., Human Amyloid Imaging 2017). In summary, current evidence supports the use of reference tissue approaches for quantifying tau radioligand binding, obliterating the need for arterial blood sampling in clinical studies. According to some reports, SUVr may lead to a time-dependent bias, and reference tissue models applied on dynamic data may therefore be considered a possible compromise between clinical feasibility and accuracy.

## 5. METHODS

To investigate the current studies in which imaging of tau was performed in dementia patients; a literature search was carried out using the following search terms: ((Dementia OR Alzheimer\* OR mild cognitive impairment OR Parkinson\* OR front\* OR vascular OR Lewy body disease) AND (tau OR neurofibrillary tangles) AND (PET OR imaging OR Neuroimaging)). Using the above



search strategy 1618 titles and abstracts were identified on 26<sup>th</sup> August 2016 (BH) – 31st December 2016 (EM). These papers were screened on the basis of relevance of title and abstract to the review. To be included articles had to be written in English and the studies had to use *in vivo* neuroimaging of tau in human dementia patients. Greater weight will be ascribed to studies with more than 5 subject per group compared to single-case studies. To ensure that all relevant references were sourced, references were in turn reviewed for other relevant articles.

## **6. RESULTS**

### ***6.1. Normal ageing***

Several studies have characterised the *in vivo* pattern of tau pathology in cognitively normal older subjects. Focal uptake has been observed in the medial temporal lobe structures (Table 1; Figure 2), including the entorhinal cortex, parahippocampal gyrus and hippocampus (Ossenkoppele et al., 2016; Smith et al., 2016b). Limited tau localisations in medial and inferior temporal regions were also reported, corresponding with Braak stage III/IV (Johnson et al., 2016). Interestingly, these findings were extended by another study revealing a differential topography of tau accumulation according to amyloid status (Schöll et al., 2016). Consistent with previous studies (Johnson et al., 2016; Ossenkoppele et al., 2016), amyloid-negative subjects showed focal uptake in the medial temporal lobe whereas amyloid-positive subjects had a wider distribution involving the inferior and lateral temporal lobes as well as the posterior cingulate cortex (Schöll et al., 2016). It is noteworthy that tau burden in these structures were strongly correlated with increasing age (Johnson et al., 2016; Schöll et al., 2016). Whether these regionally-specific associations constitute primary age-related tauopathy (PART) remains a topic of future investigation (Crary et al., 2014).

## **6.2. Mild cognitive impairment and Alzheimer's disease**

At present, the majority of tau PET imaging studies have focussed on patients with MCI and AD (Chiotis et al., 2016; Cho et al., 2016a, 2016b; Harada et al., 2015a; Ishiki et al., 2015a; Johnson et al., 2016; Kimura et al., 2015; Okamura et al., 2014; Ossenkuppele et al., 2016; Schöll et al., 2016; Schwarz et al., 2016; Villemagne et al., 2014). Elevated tau accumulation in predominantly temporo-parietal cortices has been consistently reported in AD (Figure 2), leading to excellent discrimination from healthy controls, (Chiotis et al., 2016; Harada et al., 2015a, 2015c; Okamura et al., 2014; Villemagne et al., 2014). Furthermore, the regional topography of *in vivo* tau accumulation is strikingly consistent across various radioactive tracers and parallel closely with post-mortem spreading patterns of NFTs and neurodegeneration (Braak and Braak, 1991; Schwarz et al., 2016; Villemagne et al., 2014).

Somewhat surprisingly, increased hippocampal tau binding in AD relative to controls has not been robustly reported (Harada et al., 2015a; Johnson et al., 2016). This could be attributed to a number of factors: (a) both tau PET imaging and histopathological data have frequently shown focal hippocampal and transenthorinal tau accumulation in the non-demented elderly population (Kuzuhara et al., 1989), (b) signal from “off-target” binding in the choroid plexus may spill into the hippocampus, thereby diminishing group differences or (c) limited resolution of PET imaging to localise ligand binding within the hippocampus, resulting in an underestimation of PET signal in patient groups where substantial atrophy is present.

To date, there is only one longitudinal report of tau progression in AD (Ishiki et al., 2015b), although several large-scale studies are ongoing. Using the [<sup>18</sup>F]THK5117 tracer, Ishikii and colleagues have investigated the accumulation of tau over 1.2 – 1.5 years in a small sample of 5

AD and 5 age-matched healthy controls. The AD group showed significantly greater annual increase of tau burden in the middle and inferior temporal cortices (+4.98%) and in the fusiform gyrus (+5.2%) compared to 2% in the control group, which also correlated with the rate of cognitive decline. Further longitudinal studies with larger samples and analyses of test-retest reliability of tau PET quantification are warranted to replicate this finding.

Compared to the diffuse pattern of tau in AD, MCI appears to be characterised with a more focal pattern of tau burden in entorhinal regions (Chiotis et al., 2016; Cho et al., 2016b). Group comparisons between MCI and AD have yielded inconsistent findings of no significant differences (Chiotis et al., 2016) and increased tau burden in AD (Cho et al., 2016b). Divergent spreading patterns of tau and amyloid in a relatively large sample (53 AD, 75 MCI and 67 healthy controls) were also reported (Cho et al., 2016a). Consistent with neuropathological data, amyloid pathology was present in diffuse regions throughout the neocortex while tau accumulation was frequently localised to the medial temporal lobe region and progressed in a step-wise fashion to other temporo-parietal regions and the posterior cingulate cortex (Cho et al., 2016a).

Histopathological and CSF studies have described strong correlations between tau pathology and cognitive impairment (Han et al., 2012; Van Rossum et al., 2012). In this regard, *in vivo* tau PET imaging has greatly expanded our interpretations of the CSF-cognition correlations by providing additional spatial information at the vertex-wise and regions-of-interest (ROI) scales. In one study, despite an absence of cognitive correlations with global cortical tau, increased [<sup>18</sup>F]AV1451 binding in bilateral orbitofrontal and temporal cortices were associated with poorer MMSE scores (Ossenkoppele et al., 2016). Interestingly, visuospatial performance was also correlated with increased binding in the bilateral occipital lobe and temporo-parietal cortices (Ossenkoppele et al., 2016). Numerous PET studies have reported moderate to strong correlations between tau and

cognition in MCI and AD, including visual, verbal and episodic memory function (Cho et al., 2016b; Ossenkoppele et al., 2016; Saint-Aubert et al., 2016), language (Ossenkoppele et al., 2016) as well as global cognition (Cho et al., 2016a, 2016b; Ishiki et al., 2015a; Saint-Aubert et al., 2016).

### **6.3. Frontotemporal dementia**

#### *6.3.1. MAPT-related FTD*

FTD is a progressive neurodegenerative syndrome and it is the third most common cause of degenerative dementia, accounting for between 5 – 15 % of dementia patients (Neary et al., 1998). On structural MRI, FTD is typically characterised by cortical atrophy in prefrontal and temporal cortices (Rohrer and Rosen, 2013). The MAPT gene is one of the most prevalent genes implicated in FTD and is located on chromosome 17q51. Mutation carriers often demonstrate behavioural changes, dementia and parkinsonism (Rademakers et al., 2004; Rizzu et al., 1999). To date, there are only 2 tau-PET case studies involving MAPT carriers (Bevan Jones et al., 2016; Smith et al., 2016a). Among 3 patients harbouring a p.R406W MAPT mutation, increased [<sup>18</sup>F]AV1451 retention was most evident in the temporal poles, hippocampus and the inferior temporal gyrus as well as the frontal lobe (Smith et al., 2016a). These descriptive findings were later extended by a comparative single-case study of a 10 + 16C>T MAPT mutation carrier with behavioural variant FTD (bvFTD) versus a group of 12 aged-matched healthy controls (Bevan Jones et al., 2016). The bvFTD patient demonstrated increased [<sup>18</sup>F]AV1451 uptake in anterior temporal lobes and ventral anterior cingulate cortex, both of which are regions prone to tau accumulation in FTD (Kertesz et al., 2005).

#### *6.3.2 Progressive Supranuclear Palsy*

PSP is a rare neurological disorder that is characterised by vertical gaze palsy, rigidity, instability and dementia (Steele et al., 1964). At present, there are 6 PET studies in PSP (Cho et al., 2016c;

Kepe et al., 2013; Lopera et al., 2013; Smith et al., 2016b; Whitwell et al., 2016; Passamonti et al., 2017). The first tau-PET study in PSP reported that PSP subjects (n=15) showed significantly increased [<sup>18</sup>F]FDDNP binding in several subcortical regions, particularly the subthalamic and midbrain regions, compared to age-matched healthy controls (n=5) and individuals with early-stage Parkinson's disease (PD) (n=8) (Kepe et al., 2013). Indeed, the differential tau profiles could be clinically important for differential diagnosis considering the overlapping symptoms in the early stages of PSP and PD. A subset of severe-PSP subjects also had increased tau burden in the frontal cortical regions, which was, in turn, correlated with disease severity (PSP Rating Scale). These findings have since been confirmed by recent studies using the [<sup>18</sup>F]AV1451 tracer (Smith et al., 2016b; Passamonti et al., 2017) (Figure 3). Subcortical involvement in PSP compared to age-matched controls have been reported particularly in the midbrain and the globus pallidus, putamen, caudate nucleus and thalamus (Cho et al., 2016c; Smith et al., 2016b; Whitwell et al., 2016). This is consistent with findings from two single PSP case studies which also used [<sup>18</sup>F]AV1451 (Chiotis et al., 2016; Hammes et al., 2016).

However, autoradiographic analyses of the PSP tissues (n = 3) have not revealed any specific binding of [<sup>18</sup>F]AV1451 to tau aggregates in neither the frontal cortical tissue nor in the putamen. This corroborates with previous *ex vivo* evidence suggesting negligible or suboptimal binding of [<sup>18</sup>F]AV1451 to straight tau filaments in non-AD tauopathies (Fodero-Tavoletti et al., 2014; Normandin et al., 2015; Sander et al., 2016). In summary, there is convergent *in vivo* evidence for increased tau burden in the midbrain in PSP and this agrees with the known neuropathological data (Dickson, 1999). However, poor agreement with post-mortem studies and substantial overlap with healthy controls precludes a straightforward recommendation on the clinical utility of tau PET for PSP at this stage.

#### **6.4. Lewy body diseases**

Lewy body diseases, such as dementia with Lewy bodies (DLB) and Parkinson's disease (PD) are characterised by intraneuronal inclusions of alpha-synuclein, known as Lewy bodies. DLB is the second leading cause of degenerative dementia after AD, accounting for 15% of dementia cases at autopsy. Core features of DLB include the clinical triad of parkinsonism, fluctuating cognitive impairment and recurrent visual hallucinations (McKeith et al., 2005). In addition to the hallmark pathology of Lewy bodies, DLB patients often have co-existing AD pathologies, such as extracellular amyloid plaques and NFTs (Ballard et al., 2006; Colom-Cadena et al., 2013). Despite being present at levels that are markedly lower compared to AD, there is increasing evidence to suggest that these pathologies contribute to the clinical presentation and aggravate the rates of neurodegeneration in dementia with Lewy bodies (DLB) (Nedelska et al., 2015; Sarro et al., 2016).

There have been 2 published studies on tau imaging in DLB to date (Gomperts, 2016; Kantarci et al., 2016). Gomperts and colleagues (2016) reported increased [<sup>18</sup>F]AV1451 uptake in the temporo-parietal cortices and precuneus among DLB (n=7) and PD patients with cognitive impairment (n=8) relative to amyloid-negative controls (n=29) (Gomperts et al., 2016). This pattern of increased tau uptake was also significantly correlated with MMSE scores. In contrast, PD patients with normal cognition did not show any evidence for increased tau burden. Rather intriguingly, significant tau burden was present despite minimal amyloid in the DLB group, suggesting that extensive tauopathy is possible without amyloid deposition in Lewy body diseases. With the caveat of the small sample size, this observation seemingly contrasts with the widely accepted notion that in AD, pathological spreading of tau from transentorhinal regions to other cortices occurs after an abnormal threshold of  $\beta$ -amyloid accumulation (Bloom, 2014; Stancu et al., 2014), and might instead support a growing literature suggesting a synergistic interaction between  $\alpha$ -synuclein and tau (see Moussaud et al., 2014 for a review).

Consistent with the relative preservation of the medial temporal lobe structure in DLB (Burton et al., 2009; Firbank et al., 2010; Mak et al., 2017, 2015b), [<sup>18</sup>F]AV1451 uptake showed a clear separation between DLB (maximum [<sup>18</sup>F]AV1451 SUVR in MTL = 1.33) and AD (minimum [<sup>18</sup>F]AV1451 SUVR in MTL = 1.38) (Kantarci et al., 2016). Furthermore, the regions with the highest burden of tau in the DLB group were in the occipital visual association cortices, suggesting an atypical profile of tau progression that deviates from the classical Braak staging.

## **7. RELATION OF IN VIVO TAU DEPOSITION TO OTHER MARKERS OF PATHOLOGIES**

Advances in neuroimaging methods and intra-individual registration across multimodal datasets have enabled the precise quantification of both subtle and widespread patterns of downstream neurodegeneration across the dementia spectrum, from normal aging to preclinical stages and established dementia (see Mak et al., 2016; Pini et al., 2016; Villemagne and Chételat, 2016 for a series of reviews). Briefly, there are characteristic profiles of grey and white matter changes that most likely reflect underlying differences in pathophysiology among different conditions (Mak et al., 2014; Whitwell et al., 2007). PET imaging in dementia has enabled the *in vivo* characterisation of hypometabolism (Mosconi, 2013), amyloid accumulation (O'Brien and Herholz, 2015) and tau deposition, all of which are considered to be upstream processes. The combination of these modalities allows the investigation of tau pathology in relation to other markers of pathologies and further clarifies the relationships among amyloid  $\beta$ , tau deposition and atrophy. These research endeavours have also been spurred by methodological advances. One particular example is the relatively recent implementation of surface-based approaches for smoothing of PET data, which have been demonstrated to yield less bias and higher reliability of parametric analyses compared to volumetric methods (Greve et al., 2014; Matheson et al., NRM2016)

### **7.1. Tau and structural atrophy**

Consistent with CSF studies, *in vivo* tau burden has been linked to cortical thinning and hippocampal atrophy in AD (Cho et al., 2016b; Okamura et al., 2014; Sepulcre et al., 2016; Villemagne et al., 2014; Wang et al., 2016). This is in agreement with *post-mortem* evidence showing that the density of NFTs strongly correlates with atrophy whereas  $\beta$ -amyloid does not (Burton et al., 2009; Gómez-Isla et al., 1997). Our group has also shown that the extent of tau pathology overlaps with and exceeds that of cortical atrophy in AD (Figure 4; Mak et al., Submitted to AAIC 2017). These findings collectively fit within the model that tau is intimately related to cortical atrophy as seen on MRI, a validated marker of disease progression in clinical trials. However, there are unresolved wrinkles in the relationship between tau and atrophy. In one study, the association between hippocampal tau and volume was only significant in amyloid-positive subjects (Wang et al., 2016). This intriguing finding suggests that hippocampal tau alone is insufficient in driving gross atrophy, and that additional accumulation of  $\beta$ -amyloid is necessary to potentiate tau-related atrophy in the hippocampus. While this might reflect a dose-dependent relationship between atrophy and tau that accompanies abnormal levels of amyloid, the authors did not find any significant differences in hippocampal tau between both amyloid subgroups. Alternatively, rather than increasing tau burden,  $\beta$ -amyloid may convert tau into its neurotoxic form, leading to cellular dysfunction and eventually cell death (Patel et al., 2015). There is also recent evidence that tau and amyloid could be associated with distinct spatial patterns of atrophy, in that tau is associated with local atrophy in temporal regions whereas amyloid is associated with distributed GM loss respectively (Sepulcre et al., 2016).



## **7.2. Tau and hypometabolism**

As described, hyperphosphorylation of tau results in synaptic dysfunction and eventual neuronal death. Consequently, these processes induce a reduction in neuronal energy demand or hypometabolism, which can be quantified using PET imaging with [<sup>18</sup>F]-2-fluorodeoxy-D-glucose (FDG) tracer (Sokoloff, 1981). There is concordant evidence for an inverse coupling between tau and hypometabolism in spatially overlapping regions (Chiotis et al., 2016; Lemoine et al., 2015; Ossenkoppele et al., 2016; Smith et al., 2016a, 2016c). These findings collectively confirm previous correlations between FDG-PET and CSF tau levels in AD (Ceravolo et al., 2008). In one study, AD patients showed regional correlations between [<sup>18</sup>F]THK5317 and [<sup>18</sup>F]FDG-PET in prefrontal cortices and the precuneus (Chiotis et al., 2016), suggesting that hypometabolism could be related to propagation of tau pathology beyond the medial temporal lobe. This notion would be consistent with conceptual models postulating that tau spreading precedes hypometabolism by interfering with microtubule stabilisation, impaired axonal transport, and eventually synaptic and neuronal dysfunction (Jack et al., 2013).

## **8. SUMMARY AND FUTURE DIRECTIONS**

This systematic review summarises the current literature on the novel and rapidly developing area of tau PET imaging in dementia and tauopathies. In general, anatomical patterns of tau accumulation recapitulate post-mortem topography of NFTs correlate with cognitive domains as well as other established markers of neurodegeneration, such as volumetric atrophy and regional hypometabolism. However, there are still unresolved concerns about off-target binding and imperfect mapping with post-mortem data, particularly in non-AD tauopathies. In the next section, we discuss several future directions in tau PET research, focusing on longitudinal design in preclinical dementia, multi-modal investigations, and validation studies of tau radiotracers.

### **8.1. Longitudinal tau imaging in preclinical dementia**

To date, there is only 1 published longitudinal study, although several large-scale studies are ongoing (e.g. Harvard Aging Brain Study and others). Further studies are needed to clarify the natural history of tau propagation and its effect across the spectrum from normal aging, preclinical stages to MCI and finally AD. It is now established that structural atrophy (Mak et al., 2016) and amyloid accumulation (Chetelat et al., 2013) could occur a decade before clinical onset of symptoms in dementia. In a similar – and perhaps more insightful – vein, serial tau PET will be useful in the preclinical dementia stages for a number of purposes: (a) characterising the spatio-temporal accumulation of tau in the absence of neurodegenerative or cerebrovascular factors, (b) determine early predictors of cognitive decline and disease progression, and (c) perform disease-staging within vulnerable subgroups of ApoE 4 carriers, FAD mutation carriers, or individuals with a positive family history of dementia. Longitudinal tau imaging will also allow assessment of target-engagement and serve as an outcome measure of the effectiveness of anti-tau therapies (Wischik and Staff, 2009; Yanamandra et al., 2015). However, a necessary prerequisite for these studies is to establish test-retest variability for tau radioligands. Recently, THK 5317 was shown to exhibit low within-individual variability (1-4%) in five dementia patients (Chiotis et al., 2016)

### **8.2. Mapping tau pathology to other pathological markers**

Multi-modal studies have a tremendous capacity to establish *if* and *how* tau accumulation relates to amyloid and other imaging markers (i.e. MRI, diffusion imaging, FLAIR, functional MRI). This will clarify the temporal sequence of the neurodegenerative cascade and help to detangle the relative contributions of each marker to clinical features and cognitive decline. These markers might be used in conjunction with CSF, FDG-PET and structural MRI to facilitate a fine-grained stratification of at-risk individuals, such as the recently proposed A/T/N classification scheme (Jack et al., 2016).

### 8.2.1. *Tau and white matter changes*

As discussed in this review, previous studies have reported associations of local tau burden with regional atrophy (Cho et al., 2016b; Okamura et al., 2014; Sepulcre et al., 2016; Villemagne et al., 2014; Wang et al., 2016) and hypometabolism (Chiotis et al., 2016; Lemoine et al., 2015; Ossenkoppele et al., 2016; Smith et al., 2016a, 2016c). However, the impact of tau pathology in the white matter remains unexplored despite recent *post-mortem* evidence implicating cortical tau as a strong predictor of white matter hyperintensities (WMHs) (McAleese et al., 2015). Lending further support to these autopsy findings, preliminary findings from our group indicated an age-independent association between [<sup>18</sup>F]AV1451 uptake in the parietal lobe and WMHs across a sample of healthy controls, MCI and AD (Gabel and Mak et al., submitted to AAIC 2017). Future work involving DTI and FLAIR sequences will enable the mapping of tau deposition onto white matter tracts and structural networks.

### 8.2.2. *Tau and neuroinflammation*

Neuroinflammation is an active process that is proposed to play a key role in the pathophysiology of neurodegenerative disorders. Using PET and radioligands for the 18kD Translocator Protein (TSPO), which is expressed in microglia and astrocytes, immune activation has been investigated in both preclinical and clinical stages of dementia (Fan et al., 2014; Heneka et al., 2015; Stefaniak and O'Brien, 2015; Surendranathan et al., 2015). Furthermore it is increasingly recognised that microglial activation could promote the hyperphosphorylation of tau and is an early event in mouse models of tauopathy (Bhaskar et al., 2010; Yoshiyama et al., 2007). Several efforts are underway to investigate neuroinflammatory processes in the presence of tau and other downstream pathologies by mapping the co-localisations of tau pathology with neuroinflammation and amyloid burden within the same subjects (Bevan-Jones et al., 2017)

### **8.3. Reconciliation of *in vivo* tau PET with post-mortem samples**

Firstly, for tau PET to be accepted as a clinical biomarker of tau pathology, it is necessary to verify whether the amount and spatial extent of radiotracer uptake tallies with the severity of NFTs in the brain. At present, most of the tau radiotracers exhibit variable degrees and regional off-target binding. The discrepancies between *in vivo* and post-mortem analyses are most pronounced in non-AD tauopathies and further highlight the ongoing need for more validation studies. Although several tracers have been validated in post-mortem samples (Chien et al., 2013; Harada et al., 2015a; Maruyama et al., 2013b), the brain tissues were not taken from the same subjects who had undergone *in vivo* PET imaging. It is currently difficult to determine which of the tracers may be most useful going forward as no direct comparison study has taken place. Alternatively, it might not be necessary to make such a choice as certain tracers may be preferential for different tauopathies depending upon pharmacokinetics across brain regions and the distribution of other pathological proteins that may interact with tau binding (Okamura et al., 2015). In addition, the test-retest reproducibility of tau quantification methods will have to be evaluated before longitudinal tau PET can be used for monitoring therapeutic response or disease progression (Devous et al., 2014).

## **9. CONCLUSION**

Tau-selective radiotracers have enabled the characterisation of tau burden in the living brain, hitherto possible only from post-mortem brains. There is tremendous potential for tau imaging to provide novel information about the earliest events in the pathophysiological cascade of AD and other dementias. Tau PET has great potential to contribute to the early and differential diagnosis, and longitudinal tracking with serial PET will clarify its natural history across the spectrum from normal aging to dementia, and promote efforts to developments of anti-tau interventions.

**COMPETING INTERESTS**

None declared.

**AUTHORS' CONTRIBUTIONS**

Benjamin Hall and Elijah Mak wrote the paper and conducted the literature searches.

Simon Cervenka reviewed the drafts, and contributed to the writing of the sections with regards to quantification of tau radiotracer uptake.

Franklin Aigbirhio and James Rowe reviewed the manuscript and provided critical feedback.

John O'Brien is the principal investigator of the NIMROD study, provided critical feedback, and made revisions on the manuscript.

**ACKNOWLEDGEMENTS**

We would like to the reviewers for their suggestions to improve the manuscript. The study is supported by the UK National Institute of Health Research Cambridge Biomedical Research Centre and Biomedical Research Unit in Dementia. JBR is supported by the Wellcome Trust (103838). EM is in receipt of a Gates Cambridge scholarship and an Alzheimer's Research UK Research Grant.



## FIGURES AND TABLES

	<b>Spatial topography</b>	<b>Group differences</b>	<b>Clinical and cognitive correlations</b>
<b>Normal aging</b>	Limited and focal tau deposition in medial temporal lobe structures.  Might represent primary age-related tauopathy.	Compared to amyloid-negative individuals, amyloid-positive individuals show a wider extent of tau that involves the temporo-parietal cortices.	Strongly correlated with aging.  Local tau burden in Braak I/II regions were correlated with episodic memory and retrospective longitudinal decline in episodic memory and global cognition.
<b>Mild cognitive impairment and Alzheimer's disease</b>	Parallel with neuropathological patterns of the neurofibrillary tangles.  Widespread neocortical regions extending from the temporal lobe towards the parietal cortices and precuneus, with relative sparing of motor regions.	Elevated tau burden in temporo-parietal cortices compared to controls.  Increased hippocampal binding relative to controls has not been consistently reported.	MMSE, episodic memory, visuospatial domain and language.  Closely related to atrophy and hypometabolism.
<b>Progressive supranuclear palsy</b>	Preferential uptake in subcortical rather than cortical regions.	Significant increase in the basal ganglia, midbrain, and other subcortical structures including the thalamus and putamen compared to controls.	Tau accumulation in the globus pallidus was correlated with the PSP rating scale.
<b>Lewy body diseases</b>	Posterior regions including the temporo-parietal cortex, precuneus and occipital regions.	DLB and PD subjects with cognitive impairment had increased tau uptake in inferior temporal gyrus and precuneus compared to controls.  Tau deposition in the MTL separated AD from DLB.	Increased tau in inferior temporal gyrus and precuneus was correlated with MMSE and CDR.

**Table 1. Principal findings from *in vivo* tau PET studies across various neurodegenerative conditions.** Abbreviations: AD = Alzheimer's disease, DLB = Dementia with Lewy bodies, PD =

Parkinson's disease, MMSE = Mini-Mental State Examination, CDR = Clinical Dementia Rating; MTL = medial temporal lobe.

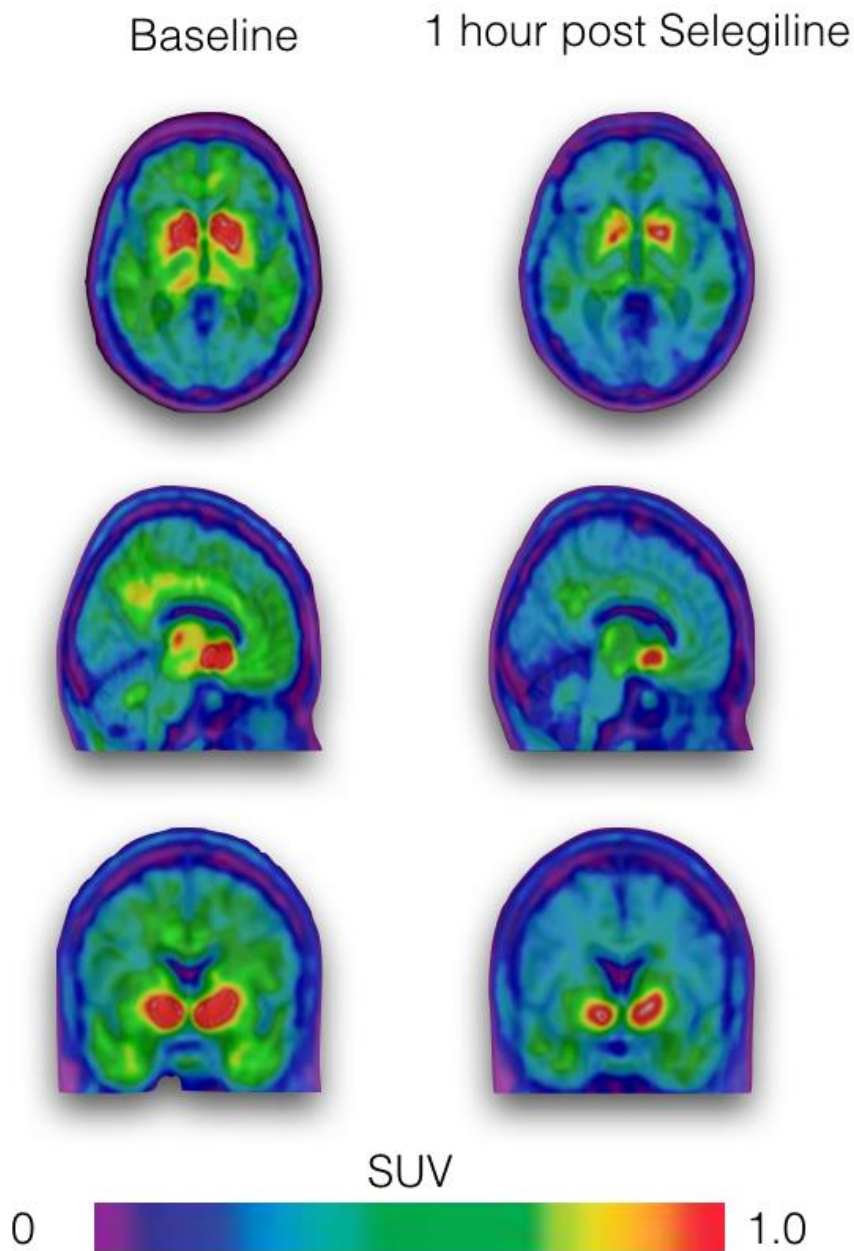


**Figure 1. Selegiline reduces  $[^{18}\text{F}]\text{THK-5351}$  uptake.** Marked reduction of uptake was observed 1 hour after 10mg Selegiline in a patient (71 years old female). Provided with courtesy from Kok Pin Ng (Presented at Human Amyloid Imaging 2017).



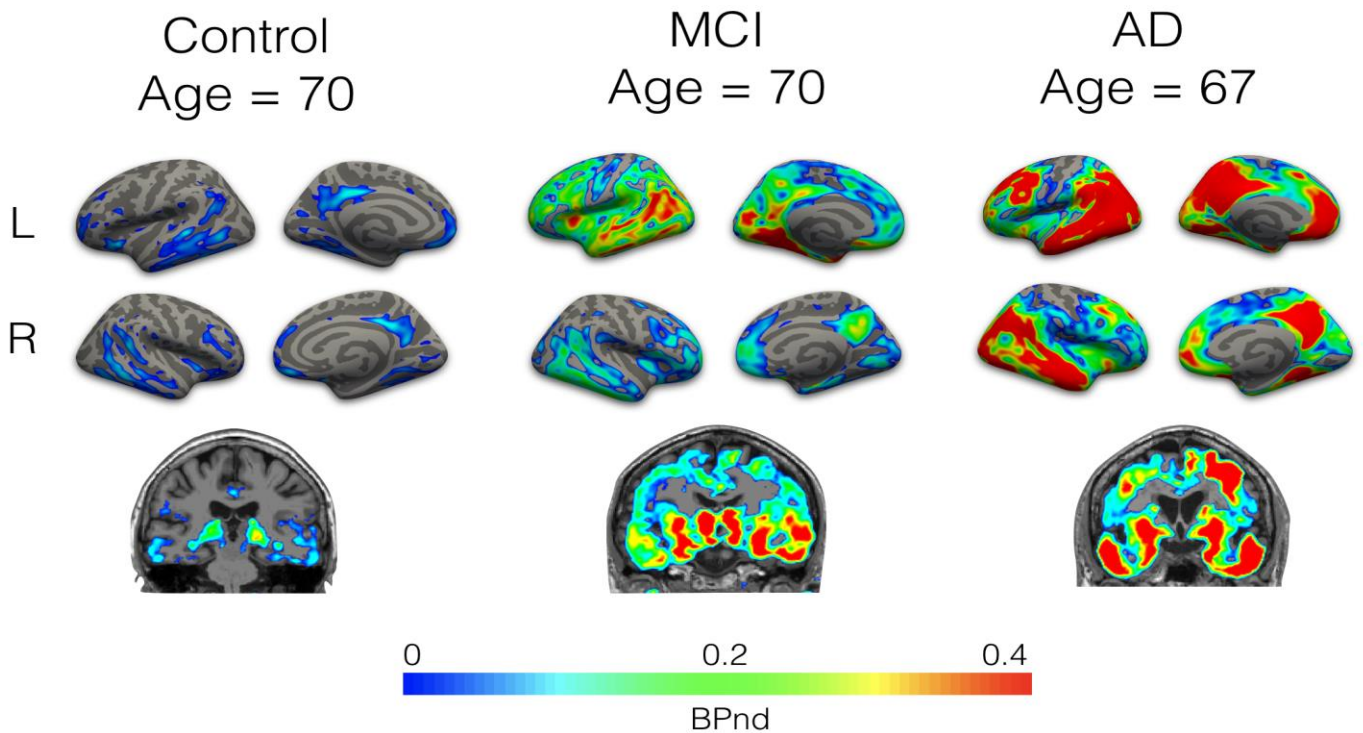


**Figure 2. Visualizing the progressive extent of  $[^{18}\text{F}]\text{AV1451}$  retention on the cortex across the spectrum of normal aging, mild cognitive impairment and Alzheimer's disease.** Consistent with the neuropathological progression of tau deposition, several studies have identified focal tau accumulation in cognitively normal adults, most prominently in the medial temporal lobe structures (Left). In contrast, mild cognitive impairment is characterised with increased uptake in the temporal and posterior cingulate regions (Middle), before progressively spreading widely across the temporo-parietal cortices in AD (Right). Volumetric data of representative subjects are represented in radiological convention. This figure is based on our data from the ongoing NIMROD study (Bevan-Jones et al., 2017).

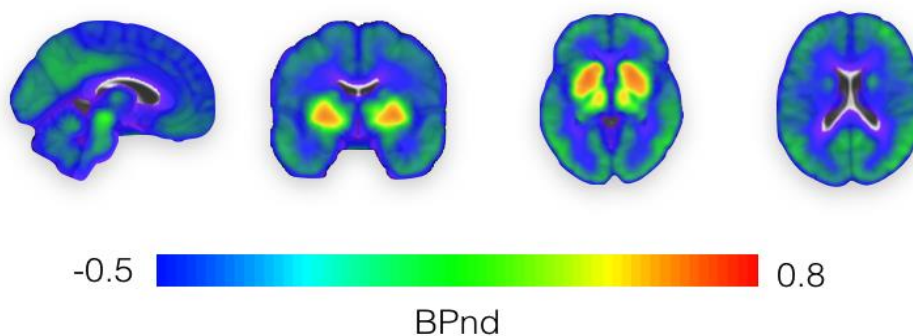


**Figure 3. Increased  $[^{18}\text{F}]\text{AV1451}$  retention in midbrain and subcortical structures in PSP at the group-averaged level (Passamonti et al., 2017).** Similarly, other studies have consistently reported increased tau deposition in the globus pallidus, putamen, caudate nucleus and thalamus.

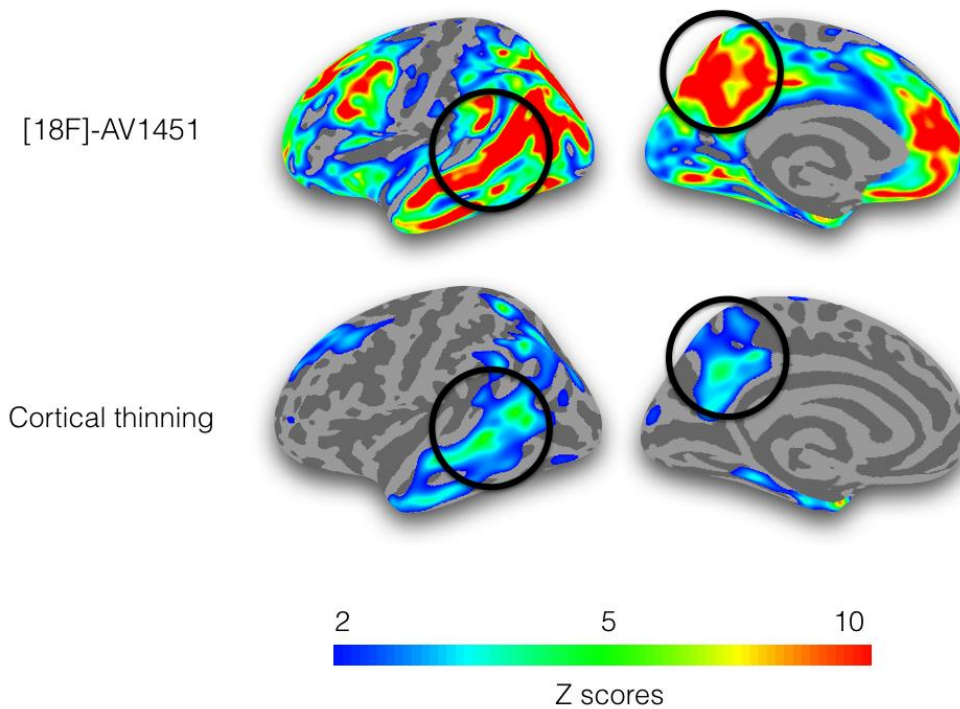


**Figure 4. Mapping the extent of tau pathology and cortical atrophy in an AD subject.** Preliminary work from our group has demonstrated that tau pathology (quantified as Z scores of [ $^{18}\text{F}$ ]AV-1451) is in excess and spatially overlaps with that of cortical thinning (inverted Z scores) in AD. In future, more multi-modal studies with intra-individual coregistrations of PET and MRI data will facilitate the investigation of tau deposition and its relationships with other downstream markers of neurodegeneration such as cortical thinning. This figure is based on our data from the ongoing NIMROD study (Bevan-Jones et al., 2017).

**REFERENCES**

- Agarwal, R., 2012. CSF tau and amyloid  $\beta$ 42 levels in Alzheimer's disease—A meta-analysis. *Adv. Alzheimer's Dis.* 1, 30–44. doi:10.4236/aad.2012.13005
- Baker, S.L., Lockhart, S.N., Price, J.C., He, M., Huesman, R.H., Schonhaut, D., Faria, J., Rabinovici, G., Jagust, W.J., 2016. Reference tissue-based kinetic evaluation of 18F-AV-1451 in aging and dementia. *J. Nucl. Med.* 57, 1–30. doi:10.2967/jnumed.116.175273
- Ballard, C., Ziabreva, I., Perry, R., Larsen, J.P., O'Brien, J., McKeith, I., Perry, E., Aarsland, D., 2006. Differences in neuropathologic characteristics across the Lewy body dementia spectrum. *Neurology* 67, 1931–4. doi:10.1212/01.wnl.0000249130.63615.cc
- Barrio, J.R., Kepe, V., Satyamurthy, N., Huang, S.C., Small, G., 2008. Amyloid and tau imaging, neuronal losses and function in mild cognitive impairment. *J. Nutr. Health Aging* 12, 61S–5S.
- Bevan-Jones, W.R., Surendranathan, A., Passamonti, L., Vázquez Rodríguez, P., Arnold, R., Mak, E., Su, L., Coles, J.P., Fryer, T.D., Hong, Y.T., Williams, G., Aigbirhio, F., Rowe, J.B., O'Brien, J.T., 2017. Neuroimaging of Inflammation in Memory and Related Other Disorders (NIMROD) study protocol: a deep phenotyping cohort study of the role of brain inflammation in dementia, depression and other neurological illnesses. *BMJ Open* 7, e013187. doi:10.1136/bmjopen-2016-013187
- Bevan Jones, W.R., Cope, T.E., Passamonti, L., Fryer, T.D., Hong, Y.T., Aigbirhio, F., Kril, J.J., Forrest, S.L., Allinson, K., Coles, J.P., Simon Jones, P., Spillantini, M.G., Hodges, J.R., O'Brien, J.T., Rowe, J.B., 2016. [18F]AV-1451 PET in behavioral variant frontotemporal dementia due to MAPT mutation. *Ann. Clin. Transl. Neurol.* doi:10.1002/acn3.366
- Bhaskar, K., Konerth, M., Kokiko-Cochran, O.N., Cardona, A., Ransohoff, R.M., Lamb, B.T., 2010. Regulation of tau pathology by the microglial fractalkine receptor. *Neuron* 68, 19–31. doi:10.1016/j.neuron.2010.08.023
- Bloom, G.S., 2014. Amyloid- $\beta$  and tau: the trigger and the bullet in Alzheimer's disease

- pathogenesis. *JAMA Neurol.* 71, 505. doi:10.1001/jamaneurol.2013.5847
- Braak, H., Braak, E., 1991. Neuropathological staging of Alzheimer-related changes. *Acta Neuropathol.* 82, 239–59.
- Braak, H., Jellinger, K., Braak, E., Bohl, J., 1992. Allocortical neurofibrillary changes in progressive supranuclear palsy. *Acta Neuropathol.* 84, 478–83.
- Brier, M.R., Gordon, B., Friedrichsen, K., McCarthy, J., Stern, A., Christensen, J., Owen, C., Aldea, P., Su, Y., Hassenstab, J., Cairns, N.J., Holtzman, D.M., Fagan, A.M., Morris, J.C., Benzinger, T.L., Ances, B.M., 2016. Tau and A-beta imaging, CSF measures, and cognition in Alzheimer's disease. *Sci. Transl. Med.* 8, 1–10. doi:10.1126/scitranslmed.aaf2362
- Burton, E.J., Barber, R., Mukaetova-Ladinska, E.B., Robson, J., Perry, R.H., Jaros, E., Kalaria, R.N., O'Brien, J.T., 2009. Medial temporal lobe atrophy on MRI differentiates Alzheimer's disease from dementia with Lewy bodies and vascular cognitive impairment: a prospective study with pathological verification of diagnosis. *Brain* 132, 195–203.  
doi:10.1093/brain/awn298
- Ceravolo, R., Borghetti, D., Kiferle, L., Tognoni, G., Giorgetti, A., Neglia, D., Sassi, N., Frosini, D., Rossi, C., Petrozzi, L., Siciliano, G., Murri, L., 2008. CSF phosphorylated TAU protein levels correlate with cerebral glucose metabolism assessed with PET in Alzheimer's disease. *Brain Res. Bull.* 76, 80–84. doi:10.1016/j.brainresbull.2008.01.010
- Chetelat, G., La Joie, R., Villain, N., Perrotin, A., De La Sayette, V., Eustache, F., Vandenberghe, R., 2013. Amyloid imaging in cognitively normal individuals, at-risk populations and preclinical Alzheimer's disease. *NeuroImage Clin.* 2, 356–365. doi:10.1016/j.nicl.2013.02.006
- Chhatwal, J.P., Schultz, A.P., Marshall, G.A., Boot, B., Gomez-Isla, T., Dumurgier, J., LaPoint, M., Scherzer, C., Roe, A.D., Hyman, B.T., Sperling, R.A., Johnson, K.A., 2016. Temporal T807 binding correlates with CSF tau and phospho-tau in normal elderly. *Neurology* 87, 920–6.  
doi:10.1212/WNL.0000000000003050

- Chien, D.T., Bahri, S., Szardenings, A.K., Walsh, J.C., Mu, F., Su, M.Y., Shankle, W.R., Elizarov, A., Kolb, H.C., 2013. Early Clinical PET Imaging Results with the Novel PHF-Tau Radioligand [F-18]-T807. *J. Alzheimer's Dis.* 34, 457–468. doi:10.3233/JAD-122059
- Chiotis, K., Saint-Aubert, L., Savitcheva, I., Jelic, V., Andersen, P., Jonasson, M., Eriksson, J., Lubberink, M., Almkvist, O., Wall, A., Antoni, G., Nordberg, A., 2016. Imaging in-vivo tau pathology in Alzheimer's disease with THK5317 PET in a multimodal paradigm. *Eur. J. Nucl. Med. Mol. Imaging* 43, 1686–1699. doi:10.1007/s00259-016-3363-z
- Cho, H., Choi, J.Y., Hwang, M.S., Kim, Y.J., Lee, H.M., Lee, H.S., Lee, J.H., Ryu, Y.H., Lee, M.S., Lyoo, C.H., 2016a. In vivo cortical spreading pattern of tau and amyloid in the Alzheimer disease spectrum. *Ann. Neurol.* 80, 247–258. doi:10.1002/ana.24711
- Cho, H., Choi, J.Y., Hwang, M.S., Lee, J.H., Kim, Y.J., Lee, H.M., Lyoo, C.H., Ryu, Y.H., Lee, M.S., 2016b. Tau PET in Alzheimer disease and mild cognitive impairment. *Neurology* 87, 375–83. doi:10.1212/WNL.0000000000002892
- Cho, H., Choi, J.Y., Hwang, M.S., Lee, S.H., Ryu, Y.H., Lee, M.S., Lyoo, C.H., 2016c. Subcortical 18-F-AV-1451 binding patterns in progressive supranuclear palsy. *Mov. Disord.* 0, 1–7. doi:10.1002/mds.26844
- Colloby, S.J., Firbank, M.J., He, J., Thomas, A.J., Vasudev, A., Parry, S.W., O'Brien, J.T., 2012. Regional cerebral blood flow in late-life depression: arterial spin labelling magnetic resonance study. *Br J Psychiatry* 200, 150–155. doi:10.1192/bjp.bp.111.092387
- Colloby, S.J., Firbank, M.J., Vasudev, A., Parry, S.W., Thomas, A.J., O'Brien, J.T., 2011. Cortical thickness and VBM-DARTEL in late-life depression. *J. Affect. Disord.* 133, 158–164. doi:10.1016/j.jad.2011.04.010
- Colom-Cadena, M., Gelpi, E., Charif, S., Belbin, O., Blesa, R., Marti, M.J., Clarimon, J., Lleo, A., 2013. Confluence of alpha-synuclein, tau, and beta-amyloid pathologies in dementia with Lewy bodies. *J. Neuropathol. Exp. Neurol.* 72, 1203–1212.

doi:10.1097/NEN.000000000000018

Crary, J.F., Trojanowski, J.Q., Schneider, J.A., Abisambra, J.F., Abner, E.L., Alafuzoff, I., Arnold, S.E., Attems, J., Beach, T.G., Bigio, E.H., Cairns, N.J., Dickson, D.W., Gearing, M., Grinberg, L.T., Hof, P.R., Hyman, B.T., Jellinger, K., Jicha, G.A., Kovacs, G.G., Knopman, D.S., Kofler, J., Kukull, W.A., Mackenzie, I.R., Masliah, E., McKee, A., Montine, T.J., Murray, M.E., Neltner, J.H., Santa-Maria, I., Seeley, W.W., Serrano-Pozo, A., Shelanski, M.L., Stein, T., Takao, M., Thal, D.R., Toledo, J.B., Troncoso, J.C., Vonsattel, J.P., White, C.L., Wisniewski, T., Woltjer, R.L., Yamada, M., Nelson, P.T., 2014. Primary age-related tauopathy (PART): a common pathology associated with human aging. *Acta Neuropathol.* 128, 755–766.

doi:10.1007/s00401-014-1349-0

Devous, M.D., Joshi, A.D., Navitsky, M.A., Dickson, J., Pontecorvo, M.A., Siderowf, A., Mintun, M.A., 2014. Test-retest data for the tau PET imaging agent of 18F-AV-1451. *Alzheimer's Dement.* 10, P901. doi:10.1016/j.jalz.2014.07.085

Dickson, D.W., 1999. Neuropathologic differentiation of progressive supranuclear palsy and corticobasal degeneration. *J. Neurol.* 116-15.

Fan, Z., Aman, Y., Ahmed, I., Chetelat, G., Landeau, B., Ray Chaudhuri, K., Brooks, D.J., Edison, P., 2014. Influence of microglial activation on neuronal function in Alzheimer's and Parkinson's disease dementia. *Alzheimers. Dement.* 1–14. doi:10.1016/j.jalz.2014.06.016

Firbank, M.J., Blamire, A.M., Teodorczuk, A., Teper, E., Burton, E.J., Mitra, D., O'Brien, J.T., 2010. High resolution imaging of the medial temporal lobe in Alzheimer's disease and dementia with Lewy bodies. *J. Alzheimers. Dis.* 21, 1129–40. doi:10.3233/JAD-2010-100138

Firbank, M.J., Lloyd, J., O'Brien, J.T., 2015. The relationship between hallucinations and FDG-PET in dementia with Lewy bodies. *Brain Imaging Behav.* doi:10.1007/s11682-015-9434-0

Fodero-Tavoletti, M.T., Furumoto, S., Taylor, L., McLean, C.A., Mulligan, R.S., Birchall, I., Harada, R., Masters, C.L., Yanai, K., Kudo, Y., Rowe, C.C., Okamura, N., Villemagne, V.L., 2014.

Assessing THK523 selectivity for tau deposits in Alzheimer's disease and non-Alzheimer's disease tauopathies. *Alzheimers. Res. Ther.* 6, 11. doi:10.1186/alzrt240

Fodero-Tavoletti, M.T., Okamura, N., Furumoto, S., Mulligan, R.S., Connor, A.R., McLean, C.A., Cao, D., Rigopoulos, A., Cartwright, G.A., O'Keefe, G., Gong, S., Adlard, P.A., Barnham, K.J., Rowe, C.C., Masters, C.L., Kudo, Y., Cappai, R., Yanai, K., Villemagne, V.L., 2011. 18F-THK523: A novel in vivo tau imaging ligand for Alzheimer's disease. *Brain* 134, 1089–1100. doi:10.1093/brain/awr038

Frisoni, G.B., Fox, N.C., Jack, C.R., Scheltens, P., Thompson, P.M., 2010. The clinical use of structural MRI in Alzheimer disease. *Nat. Rev. Neurol.* 6, 67–77. doi:10.1038/nrneurol.2009.215

Giannakopoulos, P., Herrmann, F.R., Bussière, T., Bouras, C., Kövari, E., Perl, D.P., Morrison, J.H., Gold, G., Hof, P.R., 2003. Tangle and neuron numbers, but not amyloid load, predict cognitive status in Alzheimer's disease. *Neurology* 60, 1495–500.

Gómez-Isla, T., Hollister, R., West, H., Mui, S., Growdon, J.H., Petersen, R.C., Parisi, J.E., Hyman, B.T., 1997. Neuronal loss correlates with but exceeds neurofibrillary tangles in Alzheimer's disease. *Ann. Neurol.* 41, 17–24. doi:10.1002/ana.410410106

Gomperts, S.N., J.J.L.S.J.M.A.S.C.C.N.V.R.S.J.H.G.B.C.D.K.J., 2016. Tau Positron Emission Tomographic Imaging in Lewy Body Diseases. *JAMA Neurol.* 72, 1–8. doi:10.1001/jamaneurol.2016.3338

Gomperts, S.N., Locascio, J.J., Makaretz, S.J., Schultz, A., Caso, C., Vasdev, N., Sperling, R., Growdon, J.H., Dickerson, B.C., Johnson, K., 2016. Tau Positron Emission Tomographic Imaging in the Lewy Body Diseases. *JAMA Neurol.* doi:10.1001/jamaneurol.2016.3338

Greve, D.N., Svarer, C., Fisher, P.M., Feng, L., Hansen, A.E., Baare, W., Rosen, B., Fischl, B., Knudsen, G.M., 2014. Cortical surface-based analysis reduces bias and variance in kinetic modeling of brain PET data. *Neuroimage* 92, 225–236.

doi:10.1016/j.neuroimage.2013.12.021

Hahn, A., Schain, M., Erlandsson, M., Sjolín, P., James, G.M., Strandberg, O.T., Hagerstrom, D., Lanzenberger, R., Jogi, J., Olsson, T.G., Smith, R., Hansson, O., 2016. Modeling strategies for quantification of in vivo <sup>18</sup>F-AV1451 binding in patients with tau pathology. *J. Nucl. Med.* doi:10.2967/jnumed.116.174508

Hammes, J., Bischof, G.N., Giehl, K., Faber, J., Drzezga, A., Klockgether, T., van Eimeren, T., 2016. Elevated in vivo [<sup>18</sup>F]-AV-1451 uptake in a patient with progressive supranuclear palsy. *Mov. Disord.* 0, 1–2. doi:10.1002/mds.26727

Han, S.D., Gruhl, J., Beckett, L., Dodge, H.H., Stricker, N.H., Farias, S., Mungas, D., Alzheimer's Disease Neuroimaging Initiative, the A.D.N., 2012. Beta amyloid, tau, neuroimaging, and cognition: sequence modeling of biomarkers for Alzheimer's Disease. *Brain Imaging Behav.* 6, 610–20. doi:10.1007/s11682-012-9177-0

Harada, R., Okamura, N., Furumoto, S., Furukawa, K., Ishiki, A., Tomita, N., Hiraoka, K., Watanuki, S., Shidahara, M., Miyake, M., Ishikawa, Y., Matsuda, R., Inami, A., Yoshikawa, T., Tago, T., Funaki, Y., Iwata, R., Tashiro, M., Yanai, K., Arai, H., Kudo, Y., 2015a. [<sup>18</sup>F]THK-5117 PET for assessing neurofibrillary pathology in Alzheimer's disease. *Eur. J. Nucl. Med. Mol. Imaging* 42, 1052–1061. doi:10.1007/s00259-015-3035-4

Harada, R., Okamura, N., Furumoto, S., Furukawa, K., Ishiki, A., Tomita, N., Tago, T., Hiraoka, K., Watanuki, S., Shidahara, M., Miyake, M., Ishikawa, Y., Matsuda, R., Inami, A., Yoshikawa, T., Funaki, Y., Iwata, R., Tashiro, M., Yanai, K., Arai, H., Kudo, Y., 2015b. <sup>18</sup>F-THK5351: A Novel PET Radiotracer for Imaging Neurofibrillary Pathology in Alzheimer's Disease. *J. Nucl. Med.* 57, 1–43. doi:10.2967/jnumed.115.164848

Harada, R., Okamura, N., Furumoto, S., Furukawa, K., Ishiki, A., Tomita, N., Tago, T., Hiraoka, K., Watanuki, S., Shidahara, M., Miyake, M., Ishikawa, Y., Matsuda, R., Inami, A., Yoshikawa, T., Funaki, Y., Iwata, R., Tashiro, M., Yanai, K., Arai, H., Kudo, Y., 2015c. <sup>18</sup>F-THK5351: A



- Novel PET Radiotracer for Imaging Neurofibrillary Pathology in Alzheimer's Disease. *J. Nucl. Med.* 57, 1–43. doi:10.2967/jnumed.115.164848
- Harada, R., Okamura, N., Furumoto, S., Tago, T., Yanai, K., Arai, H., Kudo, Y., 2016. Characteristics of Tau and Its Ligands in PET Imaging. *Biomolecules* 6, 7. doi:10.3390/biom6010007
- Hardy, J., Selkoe, D.J., 2002. The amyloid hypothesis of Alzheimer's disease: progress and problems on the road to therapeutics. *Science* 297, 353–356. doi:10.1126/science.1072994
- Hashimoto, H., Kawamura, K., Igarashi, N., Takei, M., Fujishiro, T., Aihara, Y., Shiomi, S., Muto, M., Ito, T., Furutsuka, K., Yamasaki, T., Yui, J., Xie, L., Ono, M., Hatori, A., Nemoto, K., Sahara, T., Higuchi, M., Zhang, M.-R., 2014. Radiosynthesis, Photoisomerization, Biodistribution, and Metabolite Analysis of <sup>11</sup>C-PBB3 as a Clinically Useful PET Probe for Imaging of Tau Pathology. *J. Nucl. Med.* 55, 1532–1539. doi:10.2967/jnumed.114.139550
- Heneka, M.T., Carson, M.J., Khoury, J. El, Landreth, G.E., Brosseron, F., Feinstein, D.L., Jacobs, A.H., Wyss-Coray, T., Vitorica, J., Ransohoff, R.M., Herrup, K., Frautschy, S. a, Finsen, B., Brown, G.C., Verkhratsky, A., Yamanaka, K., Koistinaho, J., Latz, E., Halle, A., Petzold, G.C., Town, T., Morgan, D., Shinohara, M.L., Perry, V.H., Holmes, C., Bazan, N.G., Brooks, D.J., Hunot, S., Joseph, B., Deigendesch, N., Garaschuk, O., Boddeke, E., Dinarello, C. a, Breitner, J.C., Cole, G.M., Golenbock, D.T., Kummer, M.P., 2015. Neuroinflammation in Alzheimer's disease. *Lancet Neurol.* 14, 388–405. doi:10.1016/S1474-4422(15)70016-5
- Hostetler, E.D., Walji, A.M., Zeng, Z., Miller, P., Bennacef, I., Salinas, C., Connolly, B., Gantert, L., Haley, H., Holahan, M., Purcell, M., Riffel, K., Lohith, T.G., Coleman, P., Soriano, A., Ogawa, A., Xu, S., Zhang, X., Joshi, E., Della Rocca, J., Hesk, D., Schenk, D.J., Evelhoch, J.L., 2016. Preclinical Characterization of <sup>18</sup>F-MK-6240, a Promising PET Tracer for In Vivo Quantification of Human Neurofibrillary Tangles. *J. Nucl. Med.* 57, 1599–1606. doi:10.2967/jnumed.115.171678

- Ikonomovic, M.D., Abrahamson, E.E., Price, J.C., Mathis, C.A., Klunk, W.E., 2016. [F-18]AV-1451 PET retention in choroid plexus: More than "off-target" binding. *Ann. Neurol.* 8, 2–3. doi:10.1002/ana.24706
- Innis, R.B., Cunningham, V.J., Delforge, J., Fujita, M., Gjedde, A., Gunn, R.N., Holden, J., Houle, S., Huang, S.-C., Ichise, M., Iida, H., Ito, H., Kimura, Y., Koeppe, R. a, Knudsen, G.M., Knuuti, J., Lammertsma, A. a, Laruelle, M., Logan, J., Maguire, R.P., Mintun, M. a, Morris, E.D., Parsey, R., Price, J.C., Slifstein, M., Sossi, V., Suhara, T., Votaw, J.R., Wong, D.F., Carson, R.E., 2007. Consensus nomenclature for in vivo imaging of reversibly binding radioligands. *J. Cereb. Blood Flow Metab.* 27, 1533–9. doi:10.1038/sj.jcbfm.9600493
- Ishiki, A., Okamura, N., Furukawa, K., Furumoto, S., Harada, R., Tomita, N., Hiraoka, K., Watanuki, S., Ishikawa, Y., Tago, T., Funaki, Y., Iwata, R., Tashiro, M., Yanai, K., Kudo, Y., Arai, H., 2015a. Longitudinal Assessment of Tau Pathology in Patients with Alzheimer’s Disease Using [18F]THK-5117 Positron Emission Tomography. *PLoS One* 10, e0140311. doi:10.1371/journal.pone.0140311
- Ishiki, A., Okamura, N., Furukawa, K., Furumoto, S., Harada, R., Tomita, N., Hiraoka, K., Watanuki, S., Ishikawa, Y., Tago, T., Funaki, Y., Iwata, R., Tashiro, M., Yanai, K., Kudo, Y., Arai, H., 2015b. Longitudinal Assessment of Tau Pathology in Patients with Alzheimer’s Disease Using [18F]THK-5117 Positron Emission Tomography. *PLoS One* 10, e0140311. doi:10.1371/journal.pone.0140311
- Jack, C.R., Hampel, H.J., Universities, S., Cu, M., Petersen, R.C., 2016. A / T / N : An unbiased descriptive classification scheme for Alzheimer disease biomarkers. *Neurology* 0, 1–10.
- Jack, C.R., Knopman, D.S., Jagust, W.J., Petersen, R.C., Weiner, M.W., Aisen, P.S., Shaw, L.M., Vemuri, P., Wiste, H.J., Weigand, S.D., Lesnick, T.G., Pankratz, V.S., Donohue, M.C., Trojanowski, J.Q., 2013. Tracking pathophysiological processes in Alzheimer’s disease: an updated hypothetical model of dynamic biomarkers. *Lancet Neurol.* 12, 207–216.

doi:10.1016/S1474-4422(12)70291-0

- Johnson, K.A., Schultz, A., Betensky, R.A., Becker, J.A., Sepulcre, J., Rentz, D., Mormino, E., Chhatwal, J., Amariglio, R., Papp, K., Marshall, G., Albers, M., Mauro, S., Pepin, L., Alverio, J., Judge, K., Philiostaint, M., Shoup, T., Yokell, D., Dickerson, B., Gomez-Isla, T., Hyman, B., Vasdev, N., Sperling, R., 2016. Tau positron emission tomographic imaging in aging and early Alzheimer disease. *Ann. Neurol.* 79, 110–119. doi:10.1002/ana.24546
- Jonasson, M., Wall, A., Chiotis, K., Saint-Aubert, L., Wilking, H., Sprycha, M., Borg, B., Thibblin, A., Eriksson, J., Sörensen, J., Antoni, G., Nordberg, A., Lubberink, M., 2016. Tracer Kinetic Analysis of (S)-18F-THK5117 as a PET Tracer for Assessing Tau Pathology. *J. Nucl. Med.* 57, 574–581. doi:10.2967/jnumed.115.158519
- Kantarci, K., Lowe, V.J., Boeve, B.F., Senjem, M.L., Tosakulwong, N., Lesnick, T.G., Spychalla, A.J., Gunter, J.L., Fields, J.A., Graff-Radford, J., Ferman, T.J., Jones, D.T., Murray, M.E., Knopman, D.S., Jack, C.R., Petersen, R.C., 2016. AV-1451 Tau and  $\beta$ -Amyloid PET Imaging in Dementia with Lewy Bodies. *Ann. Neurol.* 1–35. doi:10.1002/ana.24825
- Karran, E., Hardy, J., 2014. Anti-amyloid therapy for Alzheimer's disease--are we on the right road? *N. Engl. J. Med.* 370, 377–8. doi:10.1056/NEJMe1313943
- Kepe, V., Bordelon, Y., Boxer, A., Huang, S.C., Liu, J., Thiede, F.C., Mazziotta, J.C., Mendez, M.F., Donoghue, N., Small, G.W., Barrio, J.R., 2013. PET imaging of neuropathology in tauopathies: Progressive supranuclear palsy. *J. Alzheimer's Dis.* 36, 145–153. doi:10.3233/JAD-130032
- Kertesz, A., McMonagle, P., Blair, M., Davidson, W., Munoz, D.G., 2005. The evolution and pathology of frontotemporal dementia. *Brain* 128, 1996–2005. doi:10.1093/brain/awh598
- Kimura, Y., Ichise, M., Ito, H., Shimada, H., Ikoma, Y., Seki, C., Takano, H., Kitamura, S., Shinotoh, H., Kawamura, K., Zhang, M.-R., Sahara, N., Suhara, T., Higuchi, M., 2015. PET Quantification of Tau Pathology in Human Brain with 11C-PBB3. *J. Nucl. Med.* 1359–1366.

doi:10.2967/jnumed.115.160127

- Klunk, W.E., Engler, H., Nordberg, A., Wang, Y., Blomqvist, G., Holt, D.P., Bergstro, M., Savitcheva, I., Debnath, M.L., Barletta, J., Price, J.C., Sandell, J., Lopresti, B.J., Wall, A., Koivisto, P., Antoni, G., Mathis, C.A., Långstro, B., 2004. Imaging Brain Amyloid in Alzheimer's Disease with Pittsburgh Compound-B 306–319. doi:10.1002/ana.20009
- Kuzuhara, S., Ihara, Y., Toyokura, Y., Shimada, H., 1989. [A semiquantitative study on Alzheimer neurofibrillary tangles demonstrated immunohistochemically with anti-tau antibodies, in the brains of non-demented and demented old people]. *No To Shinkei* 41, 465–70.
- Lammertsma, a a, Hume, S.P., 1996. Simplified reference tissue model for PET receptor studies. *Neuroimage* 4, 153–8. doi:10.1006/nimg.1996.0066
- Lemoine, L., Saint-Aubert, L., Marutle, A., Antoni, G., Eriksson, J.P., Ghetti, B., Okamura, N., Nennesmo, I., Gillberg, P.-G., Nordberg, A., 2015. Visualization of regional tau deposits using (3)H-THK5117 in Alzheimer brain tissue. *Acta Neuropathol. Commun.* 3, 40. doi:10.1186/s40478-015-0220-4
- Logan, J., Fowler, J.S., Volkow, N.D., Wang, G.J., Ding, Y.S., Alexoff, D.L., 1996. Distribution volume ratios without blood sampling from graphical analysis of PET data. *J Cereb Blood Flow Metab* 16, 834–40.
- Logan, J., Fowler, J.S., Volkow, N.D., Wolf, A.P., Dewey, S.L., Schlyer, D.J., MacGregor, R.R., Hitzemann, R., Bendriem, B., Gatley, S.J., 1990. Graphical analysis of reversible radioligand binding from time-activity measurements applied to [N-11C-methyl]-(-)-cocaine PET studies in human subjects. *J. Cereb. Blood Flow Metab.* 10, 740–7. doi:10.1038/jcbfm.1990.127
- Lopera, F., Giraldo, M., Acosta, N., Munoz, C., Moreno, S., Tirado, V., Garcia Ospina, G.P., Langbaum, J., Ho, C., Suliman, S., Cho, W., Tariot, P., Reiman, E., 2013. Alzheimer's Prevention Initiative Colombia registry in the PSEN1 E280A mutation kindred. *Alzheimer's Dement.* 9, P321. doi:10.1016/j.jalz.2013.04.151

- Lowe, V.J., Curran, G., Fang, P., Liesinger, A.M., Josephs, K.A., Parisi, J.E., Kantarci, K., Boeve, B.F., Pandey, M.K., Bruinsma, T., Knopman, D.S., Jones, D.T., Petrucelli, L., Cook, C.N., Graff-Radford, N.R., Dickson, D.W., Petersen, R.C., Jack, C.R., Murray, M.E., 2016. An autoradiographic evaluation of AV-1451 Tau PET in dementia. *Acta Neuropathol. Commun.* 4, 58. doi:10.1186/s40478-016-0315-6
- Mak, E., Gabel, S., Mirette, H., Su, L., Williams, G.B., Waldman, A., Wells, K., Ritchie, K., Ritchie, C., O'Brien, J., 2016. Structural neuroimaging in preclinical dementia: from microstructural deficits and grey matter atrophy to macroscale connectomic changes. *Ageing Res. Rev.* doi:10.1016/j.arr.2016.10.001
- Mak, E., Gabel, S., Su, L., Williams, G.B., Arnold, R., Passamonti, L., Rodríguez, P.V., Surendranathan, A., Bevan-jones, W.R., Rowe, J.B., Brien, J.T.O., 2017. Multi-modal MRI investigation of volumetric and microstructural changes in the hippocampus and its subfields in mild cognitive impairment , Alzheimer ' s disease , and dementia with Lewy bodies 1–11. doi:10.1017/S1041610216002143
- Mak, E., Su, L., Williams, G., O'Brien, J., 2014. Neuroimaging characteristics of dementia with Lewy bodies. *Alzheimers. Res. Ther.* 6, 18.
- Mak, E., Su, L., Williams, G.B., Watson, R., Firbank, M., Blamire, A.M., O'Brien, J.T., 2015a. Longitudinal assessment of global and regional atrophy rates in Alzheimer's disease and dementia with Lewy bodies. *NeuroImage Clin.* 7, 456–462. doi:10.1016/j.nicl.2015.01.017
- Mak, E., Su, L., Williams, G.B., Watson, R., Firbank, M., Blamire, A.M., O'Brien, J.T., 2015b. Differential atrophy of hippocampal subfields: a comparative study of dementia with Lewy bodies and Alzheimer's disease. *Am. J. Geriatr. Psychiatry* 24, 136–143. doi:10.1016/j.jagp.2015.06.006
- Marquié, M., Normandin, M.D., Vanderburg, C.R., Costantino, I.M., Bien, E.A., Rycyna, L.G., Klunk, W.E., Mathis, C.A., Ikonovic, M.D., Debnath, M.L., Vasdev, N., Dickerson, B.C.,

- Gomperts, S.N., Growdon, J.H., Johnson, K.A., Frosch, M.P., Hyman, B.T., Gómez-Isla, T., 2015. Validating novel tau positron emission tomography tracer [F-18]-AV-1451 (T807) on postmortem brain tissue. *Ann. Neurol.* 78, 787–800. doi:10.1002/ana.24517
- Maruyama, M., Shimada, H., Suhara, T., Shinotoh, H., Ji, B., Maeda, J., Zhang, M.R., Trojanowski, J., Lee, V.Y., Ono, M., Masamoto, K., Takano, H., Sahara, N., Iwata, N., Okamura, N., Furumoto, S., Kudo, Y., Chang, Q., Saido, T., Takashima, A., Lewis, J., Jang, M.K., Aoki, I., Ito, H., Higuchi, M., 2013a. Imaging of tau pathology in a tauopathy mouse model and in alzheimer patients compared to normal controls. *Neuron* 79, 1094–1108. doi:10.1016/j.neuron.2013.07.037
- Maruyama, M., Shimada, H., Suhara, T., Shinotoh, H., Ji, B., Maeda, J., Zhang, M.R., Trojanowski, J., Lee, V.Y., Ono, M., Masamoto, K., Takano, H., Sahara, N., Iwata, N., Okamura, N., Furumoto, S., Kudo, Y., Chang, Q., Saido, T., Takashima, A., Lewis, J., Jang, M.K., Aoki, I., Ito, H., Higuchi, M., 2013b. Imaging of tau pathology in a tauopathy mouse model and in alzheimer patients compared to normal controls. *Neuron* 79, 1094–1108. doi:10.1016/j.neuron.2013.07.037
- McAleese, K.E., Firbank, M., Dey, M., Colloby, S.J., Walker, L., Johnson, M., Beverley, J.R., Taylor, J.P., Thomas, A.J., O'Brien, J.T., Attems, J., 2015. Cortical tau load is associated with white matter hyperintensities. *Acta Neuropathol. Commun.* 3, 60. doi:10.1186/s40478-015-0240-0
- Mckeith, I.G., Dickson, D.W., Lowe, J., Emre, M., O'Brien, J.T., Feldman, H., Cummings, J., Duda, J.E., Lippa, C., Perry, E.K., Aarsland, D., Arai, H., Ballard, C.G., Boeve, B., Burn, D.J., Costa, D., Del Ser, T., Dubois, B., Galasko, D., Gauthier, S., Goetz, C.G., Gomez-Tortosa, E., Halliday, G., Hansen, L.A., Hardy, J., Iwatsubo, T., Kalaria, R.N., Kaufer, D., Kenny, R.A., Korczyn, A., Kosaka, K., Lee, V.M., Lees, A., Litvan, I., Londos, E., Lopez, O.L., Minoshima, S., Mizuno, Y., Molina, J.A., Mukaetova-Ladinska, E.B., Pasquier, F., Perry, R.H., Schulz,

- J.B., Trojanowski, J.Q., Yamada, M., Brien, J.T.O., Feldman, H., Cummings, J., Duda, J.E., Lippa, C., Perry, E.K., Aarsland, D., 2005. Diagnosis and management of dementia with Lewy bodies: third report of the DLB Consortium. *Neurology* 65, 1863–1872.  
doi:10.1212/01.wnl.0000187889.17253.b1
- Mosconi, L., 2013. Glucose metabolism in normal aging and Alzheimer's disease: methodological and physiological considerations for PET studies. *Clin Transl Imaging* 1, 997–1003.  
doi:10.1016/j.biotechadv.2011.08.021.Secreted
- Moussaud, S., Jones, D.R., Moussaud-Lamodière, E.L., Delenclos, M., Ross, O.A., McLean, P.J., 2014. Alpha-synuclein and tau: teammates in neurodegeneration? *Mol. Neurodegener.* 9, 43.  
doi:10.1186/1750-1326-9-43
- Neary, D., Snowden, J.S., Gustafson, L., Passant, U., Stuss, D., Black, S., Freedman, M., Kertesz, A., Robert, P.H., Albert, M., Boone, K., Miller, B.L., Cummings, J., Benson, D.F., 1998. Frontotemporal lobar degeneration: a consensus on clinical diagnostic criteria. *Neurology* 51, 1546–54.
- Nedelska, Z., Ferman, T.J., Boeve, B.F., Przybelski, S.A., Lesnick, T.G., Murray, M.E., Gunter, J.L., Senjem, M.L., Vemuri, P., Smith, G.E., Geda, Y.E., Graff-Radford, J., Knopman, D.S., Petersen, R.C., Parisi, J.E., Dickson, D.W., Jack, C.R., Kantarci, K., 2015. Pattern of brain atrophy rates in autopsy-confirmed dementia with Lewy bodies. *Neurobiol. Aging*.  
doi:10.1016/j.neurobiolaging.2014.07.005
- Normandin, M.D., Vanderburg, C.R., Ba, I.M.C., Bs, E.A.B., Bs, L.G.R., Klunk, W.E., Mathis, C.A., Ikonomic, M.D., Ms, M.L.D., Vasdev, N., Dickerson, B.C., Gomperts, S.N., Growdon, J.H., Johnson, K.A., Frosch, M.P., 2015. Validating Novel Tau Positron Emission Tomography Tracer [F-18]-AV-1451 (T807) on Postmortem Brain Tissue. *Ann. Neurol.* 78, 787–800.  
doi:10.1002/ana.24517
- O'Brien, J.T., Herholz, K., 2015. Amyloid imaging for dementia in clinical practice. *BMC Med.* 13,

163. doi:10.1186/s12916-015-0404-6

Okamura, N., Furumoto, S., Fodero-Tavoletti, M.T., Mulligan, R.S., Harada, R., Yates, P., Pejoska, S., Kudo, Y., Masters, C.L., Yanai, K., Rowe, C.C., Villemagne, V.L., 2014. Non-invasive assessment of Alzheimer's disease neurofibrillary pathology using <sup>18</sup>F-THK5105 PET. *Brain* 137, 1762–1771. doi:10.1093/brain/awu064

Okamura, N., Furumoto, S., Harada, R., Tago, T., Yoshikawa, T., Fodero-Tavoletti, M.T., Mulligan, R.S., Villemagne, V.L., Akatsu, H., Yamamoto, T., Arai, H., Iwata, R., Yanai, K., Kudo, Y., 2013. Novel <sup>18</sup>F-Labeled Arylquinoline Derivatives for Noninvasive Imaging of Tau Pathology in Alzheimer Disease. *J. Nucl. Med.* 54, 1420–1427. doi:10.2967/jnumed.112.117341

Okamura, N., Harada, R., Furukawa, K., Furumoto, S., Tago, T., Yanai, K., Arai, H., Kudo, Y., 2015. Advances in the development of tau PET radiotracers and their clinical applications. *Ageing Res. Rev.* 30, 107–113. doi:10.1016/j.arr.2015.12.010

Okamura, N., Suemoto, T., Furumoto, S., Suzuki, M., Shimadzu, H., Akatsu, H., Yamamoto, T., Fujiwara, H., Nemoto, M., Maruyama, M., Arai, H., Yanai, K., Sawada, T., Kudo, Y., 2005. Quinoline and Benzimidazole Derivatives: Candidate Probes for In Vivo Imaging of Tau Pathology in Alzheimer's Disease. *J. Neurosci.* 25, 10857–10862. doi:10.1523/JNEUROSCI.1738-05.2005

Ossenkoppele, R., Schonhaut, D.R., Schö, M., Lockhart, S.N., Ayakta, N., Baker, S.L., O'neil, J.P., Janabi, M., Lazaris, A., Cantwell, A., Vogel, J., Santos, M., Miller, Z.A., Bettcher, B.M., Vessel, K.A., Kramer, J.H., Gorno-Tempini, M.L., Miller, B.L., Jagust, W.J., Rabinovici, G.D., 2016. Tau PET patterns mirror clinical and neuroanatomical variability in Alzheimer's disease 1–17. doi:10.1093/brain/aww027

Passamonti, L., Vázquez Rodríguez, P., Hong, Y.T., Allinson, K.S.J., Williamson, D., Borchert, R.J., Sami, S., Cope, T.E., Bevan-Jones, W.R., Jones, P.S., Arnold, R., Surendranathan, A., Mak, E., Su, L., Fryer, T.D., Aigbirhio, F.I., O'Brien, J.T., Rowe, J.B., 2017. <sup>18</sup>F-AV-1451



positron emission tomography in Alzheimer's disease and progressive supranuclear palsy.

Brain aww340. doi:10.1093/brain/aww340

Patel, N., Ramachandran, S., Azimov, R., Kagan, B.L., Lal, R., 2015. Ion Channel Formation by Tau Protein: Implications for Alzheimer's Disease and Tauopathies. *Biochemistry* 54, 7320–5. doi:10.1021/acs.biochem.5b00988

Pini, L., Pievani, M., Bocchetta, M., Altomare, D., Bosco, P., Cavedo, E., Galluzzi, S., Marizzoni, M., Frisoni, G.B., 2016. Brain atrophy in Alzheimer's Disease and aging. *Ageing Res. Rev.* 30, 1–24. doi:10.1016/j.arr.2016.01.002

Rademakers, R., Cruts, M., Van Broeckhoven, C., 2004. The role of tau (MAPT) in frontotemporal dementia and related tauopathies. *Hum. Mutat.* 24, 277–295. doi:10.1002/humu.20086

Rizzu, P., Van Swieten, J.C., Joosse, M., Hasegawa, M., Stevens, M., Tibben, A., Niermeijer, M.F., Hillebrand, M., Ravid, R., Oostra, B.A., Goedert, M., van Duijn, C.M., Heutink, P., 1999. High prevalence of mutations in the microtubule-associated protein tau in a population study of frontotemporal dementia in the Netherlands. *Am. J. Hum. Genet.* 64, 414–21. doi:10.1086/302256

Rohrer, J.D., Rosen, H.J., 2013. Neuroimaging in frontotemporal dementia. *Int. Rev. Psychiatry* 25, 221–9. doi:10.3109/09540261.2013.778822

Rowe, C.C., Ellis, K.A., Rimajova, M., Bourgeat, P., Pike, K.E., Jones, G., Frupp, J., Tochon-Danguy, H., Morandau, L., O'Keefe, G., Price, R., Raniga, P., Robins, P., Acosta, O., Lenzo, N., Szoëke, C., Salvado, O., Head, R., Martins, R., Masters, C.L., Ames, D., Villemagne, V.L., 2010. Amyloid imaging results from the Australian Imaging, Biomarkers and Lifestyle (AIBL) study of aging. *Neurobiol. Aging* 31(Imaging), 1275–83. doi:10.1016/j.neurobiolaging.2010.04.007

Saint-Aubert, L., Almkvist, O., Chiotis, K., Almeida, R., Wall, A., Nordberg, A., 2016. Regional tau deposition measured by [18F]THK5317 positron emission tomography is associated to

cognition via glucose metabolism in Alzheimer's disease. *Alzheimers. Res. Ther.* 8, 38.

doi:10.1186/s13195-016-0204-z

Sander, K., Lashley, T., Gami, P., Gendron, T., Lythgoe, M.F., Rohrer, J.D., Schott, J.M., Revesz, T., Fox, N.C., Arstad, E., 2016. Characterization of tau positron emission tomography tracer [18F] AV-1451 binding to postmortem tissue in Alzheimer's disease, primary tauopathies, and other dementias. *Alzheimer's Dement.* 1–9. doi:10.1016/j.jalz.2016.01.003

Sarro, L., Senjem, M.L., Lundt, E.S., Przybelski, S.A., Lesnick, T.G., Graff-Radford, J., Boeve, B.F., Lowe, V.J., Ferman, T.J., Knopman, D.S., Comi, G., Filippi, M., Petersen, R.C., Jack, C.R., Kantarci, K., 2016. Amyloid- $\beta$  deposition and regional grey matter atrophy rates in dementia with Lewy bodies. *Brain* aww193. doi:10.1093/brain/ww193

Sasamoto, A., Miyata, J., Kubota, M., Hirao, K., Kawada, R., Fujimoto, S., Tanaka, Y., Hazama, M., Sugihara, G., Sawamoto, N., Fukuyama, H., Takahashi, H., Murai, T., 2014. Global association between cortical thinning and white matter integrity reduction in schizophrenia. *Schizophr. Bull.* 40, 420–427. doi:10.1093/schbul/sbt030

Schafer, K.N., Kim, S., Matzavinos, A., Kuret, J., 2012. Selectivity requirements for diagnostic imaging of neurofibrillary lesions in Alzheimer's disease: A simulation study. *Neuroimage* 60, 1724–1733. doi:10.1016/j.neuroimage.2012.01.066

Schöll, M., Lockhart, S.N., Schonhaut, D.R., Schwimmer, H.D., Rabinovici, G.D., Correspondence, W.J.J., Schöll, M., O'neil, J.P., Janabi, M., Ossenkoppele, R., Baker, S.L., Vogel, J.W., Faria, J., Jagust, W.J., 2016. PET Imaging of Tau Deposition in the Aging Human Brain 971–982. doi:10.1016/j.neuron.2016.01.028

Schwarz, A.J., Yu, P., Miller, B.B., Shcherbinin, S., Dickson, J., Navitsky, M., Joshi, A.D., Devous, M.D., Mintun, M.S., 2016. Regional profiles of the candidate tau PET ligand <sup>18</sup>F-AV-1451 recapitulate key features of Braak histopathological stages. *Brain* aww023. doi:10.1093/brain/aww023

- Sepulcre, J., Schultz, A.P., Sabuncu, M., Gomez-Isla, T., Chhatwal, J., Becker, A., Sperling, R., Johnson, K.A., 2016. In Vivo Tau, Amyloid, and Gray Matter Profiles in the Aging Brain. *J. Neurosci.* 36, 7364–7374. doi:10.1523/JNEUROSCI.0639-16.2016
- Shcherbinin, S., Schwarz, A.J., Joshi, A.D., Navitsky, M., Flitter, M., Shankle, W.R., Devous, M.D., Mintun, M.A., 2016. Kinetics of the tau PET tracer 18F-AV-1451 (T807) in subjects with normal cognitive function, mild cognitive impairment and Alzheimers disease. *J. Nucl. Med.* 1451. doi:10.2967/jnumed.115.170027
- Siemers, E.R., Sundell, K.L., Carlson, C., Case, M., Sethuraman, G., Liu-Seifert, H., Dowsett, S.A., Pontecorvo, M.J., Dean, R.A., Demattos, R., 2015. Phase 3 solanezumab trials: Secondary outcomes in mild Alzheimer’s disease patients. *Alzheimer’s Dement.* 12, 1–11. doi:10.1016/j.jalz.2015.06.1893
- Small, G.W., Kepe, V., Ercoli, L.M., Siddarth, P., Bookheimer, S.Y., Miller, K.J., Lavretsky, H., Burggren, A.C., Cole, G.M., Vinters, H. V., Thompson, P.M., Huang, S.-C., Satyamurthy, N., Phelps, M.E., Barrio, J.R., 2006. PET of Brain Amyloid and Tau in Mild Cognitive Impairment. *N. Engl. J. Med.* 355, 2652–2663. doi:10.1056/NEJMoa054625
- Smith, R., Puschmann, A., Schöll, M., Ohlsson, T., van Swieten, J., Honer, M., Englund, E., Hansson, O., 2016a. 18F-AV-1451 tau PET imaging correlates strongly with tau neuropathology in MAPT mutation carriers. *Brain* aww163. doi:10.1093/brain/aww163
- Smith, R., Schain, M., Nilsson, C., Strandberg, O., Olsson, T., Hägerström, D., Jögi, J., Borroni, E., Schöll, M., Honer, M., Hansson, O., 2016b. Increased Basal Ganglia Binding of 18F-AV-1451 in Patients With Progressive Supranuclear Palsy. *Mov. Disord.* 0, 1–7. doi:10.1002/mds.26813
- Smith, R., Wibom, M., Olsson, T., Hägerström, D., Jögi, J., Rabinovici, G.D., Hansson, O., 2016c. Posterior accumulation of tau and concordant hypometabolism in an early-onset Alzheimer’s disease patient with presenilin-1 mutation. *J. Alzheimer’s Dis.* 51, 339–343. doi:10.3233/JAD-

151004

- Sokoloff, L., 1981. Relationships among local functional activity, energy metabolism, and blood flow in the central nervous system. *Fed. Proc.* 40, 2311–6.
- Spillantini, M.G., Goedert, M., 2013. Tau pathology and neurodegeneration. *Lancet. Neurol.* 12, 609–22. doi:10.1016/S1474-4422(13)70090-5
- Stancu, I.-C., Vasconcelos, B., Terwel, D., Dewachter, I., 2014. Models of  $\beta$ -amyloid induced Tau-pathology: the long and “folded” road to understand the mechanism. *Mol. Neurodegener.* 9, 51. doi:10.1186/1750-1326-9-51
- Steele, J., Richardson, J., Olszewski, J., 1964. Progressive supranuclear palsy. A heterogeneous degeneration involving the brain stem, basal ganglia and cerebellum with vertical gaze and pseudobulbar palsy, nuchal dystonia and dementia. *Arch. Neurol.* 10, 333–59.
- Stefaniak, J., O’Brien, J., 2015. Imaging of neuroinflammation in dementia: a review. *J. Neurol. Neurosurg. Psychiatry* 21–28. doi:10.1136/jnnp-2015-311336
- Surendranathan, A., Rowe, J.B., O’Brien, J.T., 2015. Neuroinflammation in Lewy body dementia. *Parkinsonism Relat. Disord.* 21, 1398–1406. doi:10.1016/j.parkreldis.2015.10.009
- Trojanowski, J.Q., Vandeerstichele, H., Korecka, M., Clark, C.M., Aisen, P.S., Petersen, R.C., Blennow, K., Soares, H., Simon, A., Lewczuk, P., Dean, R., Siemers, E., Potter, W.Z., Weiner, M.W., Jack, C.R., Jagust, W., Toga, A.W., Lee, V.M.Y., Shaw, L.M., 2010. Update on the biomarker core of the Alzheimer’s Disease Neuroimaging Initiative subjects. *Alzheimer’s Dement.* 6, 230–238. doi:10.1016/j.jalz.2010.03.008
- van Berckel, B.N.M., Ossenkoppele, R., Tolboom, N., Yaqub, M., Foster-Dingley, J.C., Windhorst, A.D., Scheltens, P., Lammertsma, A.A., Boellaard, R., 2013. Longitudinal amyloid imaging using <sup>11</sup>C-PiB: methodologic considerations. *J. Nucl. Med.* 54, 1570–6. doi:10.2967/jnumed.112.113654
- Van Rossum, I.A., Visser, P.J., Knol, D.L., Van Der Flier, W.M., Teunissen, C.E., Barkhof, F.,

- Blankenstein, M.A., Scheltens, P., 2012. Injury markers but not amyloid markers are associated with rapid progression from mild cognitive impairment to dementia in Alzheimer's disease. *J. Alzheimer's Dis.* 29, 319–327. doi:10.3233/JAD-2011-111694
- Villemagne, V.L., Chételat, G., 2016. Neuroimaging biomarkers in Alzheimer's disease and other dementias. *Ageing Res. Rev.* 30, 1–13. doi:10.1016/j.arr.2016.01.004
- Villemagne, V.L., Fodero-Tavoletti, M.T., Masters, C.L., Rowe, C.C., 2015. Tau imaging: Early progress and future directions. *Lancet Neurol.* 14, 114–124. doi:10.1016/S1474-4422(14)70252-2
- Villemagne, V.L., Furumoto, S., Fodero-Tavoletti, M.T., Mulligan, R.S., Hodges, J., Harada, R., Yates, P., Piguet, O., Pejoska, S., Doré, V., Yanai, K., Masters, C.L., Kudo, Y., Rowe, C.C., Okamura, N., 2014. In vivo evaluation of a novel tau imaging tracer for Alzheimer's disease. *Eur. J. Nucl. Med. Mol. Imaging* 41, 816–826. doi:10.1007/s00259-013-2681-7
- Walji, A.M., Hostetler, E.D., Selnick, H., Zeng, Z., Miller, P., Bennacef, I., Salinas, C., Connolly, B., Gantert, L., Holahan, M., O'Malley, S., Purcell, M., Riffel, K., Li, J., Balsells, J., O'Brien, J.A., Melquist, S., Soriano, A., Zhang, X., Ogawa, A., Xu, S., Joshi, E., Della Rocca, J., Hess, F.J., Schachter, J., Hesk, D., Schenk, D., Struyk, A., Babaoglu, K., Lohith, T.G., Wang, Y., Yang, K., Fu, J., Evelhoch, J.L., Coleman, P.J., 2016. Discovery of 6-(Fluoro-<sup>18</sup>F)-3-(1*H*-pyrrolo[2,3-*c*]pyridin-1-yl)isoquinolin-5-amine ([<sup>18</sup>F]-MK-6240): A Positron Emission Tomography (PET) Imaging Agent for Quantification of Neurofibrillary Tangles (NFTs). *J. Med. Chem.* 59, 4778–4789. doi:10.1021/acs.jmedchem.6b00166
- Wang, L., Benzinger, T.L., Su, Y., Christensen, J., Friedrichsen, K., Aldea, P., McConathy, J., Cairns, N.J., Fagan, A.M., Morris, J.C., Ances, B.M., 2016. Evaluation of tau imaging in staging Alzheimer disease and revealing interactions between  $\beta$ -amyloid and tauopathy. *JAMA Neurol* 73, 1070–1077. doi:10.1001/jamaneurol.2016.2078
- Wang, Y., Mandelkow, E., 2015. Tau in physiology and pathology. *Nat. Rev. Neurosci.* 17, 22–35.

doi:10.1038/nrn.2015.1

Whitwell, J.L., Jack Jr., C.R., Parisi, J.E., Knopman, D.S., Boeve, B.F., Petersen, R.C., Ferman, T.J., Dickson, D.W., Josephs, K.A., 2007. Rates of cerebral atrophy differ in different degenerative pathologies. *Brain* 130, 1148–1158. doi:10.1093/brain/awm021

Whitwell, J.L., Lowe, V.J., Tosakulwong, N., Weigand, S.D., Senjem, M.L., Schwarz, C.G., Sychalla, A.J., Petersen, R.C., Jack, C.R., Josephs, K.A., 2016. [<sup>18</sup>F]AV-1451 tau positron emission tomography in progressive supranuclear palsy. *Mov. Disord.* 0, 1–10. doi:10.1002/mds.26834

Williams, D.R., Holton, J.L., Strand, C., Pittman, A., Silva, R. De, Lees, A.J., Revesz, T., 2007. Pathological tau burden and distribution distinguishes progressive supranuclear palsy-parkinsonism from Richardson's syndrome 1566–1576. doi:10.1093/brain/awm104

Wischik, C., Staff, R., 2009. Challenges in the conduct of disease-modifying trials in AD: Practical experience from a phase 2 trial of tau-aggregation inhibitor therapy. *J. Nutr. Heal. Aging* 13, 367–369. doi:10.1007/s12603-009-0046-5

Wong, D.F., Borroni, E., Kuwabara, H., George, N., Rosenberg, P., Lyketsos, C., Resnick, S.M., Thambisetty, M., Brasic, J., Gapasin, L., Willis, W., Knust, H., Guerard, M., Belli, S., Muri, D., Carey, T., Bedding, A., Wandel, C., Hansrod, T., Honer, M., Moghekar, A., Boess, F., Albert, M.S., Shaya, E., Oh, E., Ostrowitzki, S., Dannals, R.F., Comley, R.A., 2015. First in-human PET study of 3 novel tau radiopharmaceuticals: [<sup>11</sup>C]RO6924963, [<sup>11</sup>C]RO6931643, and [<sup>18</sup>F]RO6958948. *Alzheimer's Dement.* 11, P850–P851. doi:10.1016/j.jalz.2015.08.013

Wooten, D., Guehl, N.J., Verwer, E.E., Shoup, T.M., Yokell, D.L., Zubcevik, N., Vasdev, N., Zafonte, R.D., Johnson, K.A., El Fakhri, G., Normandin, M.D., 2016. Pharmacokinetic evaluation of the tau PET radiotracer [<sup>18</sup>F]T807 ([<sup>18</sup>F]AV-1451) in human subjects. *J. Nucl. Med.* 807, 1–27. doi:10.2967/jnumed.115.170910

Xia, C.F., Arteaga, J., Chen, G., Gangadharmath, U., Gomez, L.F., Kasi, D., Lam, C., Liang, Q.,

Liu, C., Mocharla, V.P., Mu, F., Sinha, A., Su, H., Szardenings, A.K., Walsh, J.C., Wang, E., Yu, C., Zhang, W., Zhao, T., Kolb, H.C., 2013a. [(18)F]T807, a novel tau positron emission tomography imaging agent for Alzheimer's disease. *Alzheimers. Dement.* 9, 666–76.

doi:10.1016/j.jalz.2012.11.008

Xia, C.F., Arteaga, J., Chen, G., Gangadharmath, U., Gomez, L.F., Kasi, D., Lam, C., Liang, Q., Liu, C., Mocharla, V.P., Mu, F., Sinha, A., Su, H., Szardenings, A.K., Walsh, J.C., Wang, E., Yu, C., Zhang, W., Zhao, T., Kolb, H.C., 2013b. [(18)F]T807, a novel tau positron emission tomography imaging agent for Alzheimer's disease. *Alzheimers. Dement.* 9, 666–76.

doi:10.1016/j.jalz.2012.11.008

Yanamandra, K., Jiang, H., Mahan, T.E., Maloney, S.E., Wozniak, D.F., Diamond, M.I., Holtzman, D.M., David Holtzman, C.M., 2015. Anti-tau antibody reduces insoluble tau and decreases brain atrophy. *Ann. Clin. Transl. Neurol.* 2, 278–288. doi:10.1002/acn3.176

Yoshiyama, Y., Higuchi, M., Zhang, B., Huang, S.M., Iwata, N., Saido, T.C., Maeda, J., Suhara, T., Trojanowski, J.Q., Lee, V.M.Y., 2007. Synapse Loss and Microglial Activation Precede Tangles in a P301S Tauopathy Mouse Model. *Neuron* 53, 337–351.

doi:10.1016/j.neuron.2007.01.010